Received: 20 December 2024 | Revised: 24 July 2025 | Accepted: 25 July 2025

DOI: 10.1111/bph.70177

RESEARCH ARTICLE

Elucidation of the zinc binding site in KCNQ channels

Shuo Zhang[1] | Xinhe Yang[2] | Meng Yang[1] | Yixue Cao[1] | Sai Shi[3] | Nikita Gamper[1,4] | Haixia Gao[1]

[1]Department of Pharmacology, Hebei Medical University, Shijiazhuang, China

[2]CSPC ZhongQi Pharmaceutical Technology (Shijiazhuang) Co, Ltd, Shijiazhuang, Hebei, China

[3]Department of Medical and Pharmaceutical Informatics, Hebei Medical University, Shijiazhuang, China

[4]School of Biomedical Sciences, Faculty of Biological Sciences, University of Leeds, Leeds, UK

Correspondence

Haixia Gao, Department of Pharmacology, Hebei Medical University, Shijiazhuang, China.
Email: gaohx686@hebmu.edu.cn

Nikita Gamper, School of Biomedical Sciences, Faculty of Biological Sciences, University of Leeds, UK.
Email: n.gamper@leeds.ac.uk

Sai Shi, Department of Medical and Pharmaceutical Informatics, Hebei Medical University, Shijiazhuang 050017, China.
Email: shis@tju.edu.cn

Funding information

National Natural Science Foundation of China, Grant/Award Numbers: 81871027, 82404583; Biotechnology and Biological Sciences Research Council, Grant/Award Numbers: BB/V010344/1, BB/R02104X/1; Science and Technology Development Fund, Grant/Award Number: 236Z7723G; Ministry of Education of China, Grant/Award Number: NV20230001; Medical Science Data Center of Hebei Medical University

Background and Purpose: KCNQ1-5 (Kv7.1–7.5) are members of a family of voltage-gated potassium channels with prominent function in the nervous and cardiovascular systems and in epithelia. KCNQ channels are activated by intracellular free zinc, but the molecular mechanism of this effect is poorly understood and zinc binding sites within KCNQ channels are elusive.

Experimental Approach: We used patch-clamp electrophysiology, site-directed mutagenesis and computational biology to investigate the action of zinc on **KCNQ1** and its complexes with KCNE1 or KCNE3 auxiliary subunits.

Key Results: Zinc ionophores, **zinc pyrithione** (ZnPy) and pyrrolidinedithiocarbamate (PDTC), potently activated homotetrameric KCNQ1 channels. In contrast, heteromeric KCNQ1/KCNE1 and KCNQ1/KCNE3 channels were partially inhibited by ZnPy. Focussing on this difference, we identified a putative zinc coordination site in close proximity to the KCNQ1-KCNE interface and a binding site for the KCNQ channel cofactor, **phosphatidylinositol 4,5-bisphosphate** (PIP_2). The zinc coordination site in KCNQ1 contains histidines H126 and H240, and glutamic acid E170. Additional aspartic acid D242 acts as an effector site in coupling zinc binding with channel activation. The site is partially conserved with other KCNQ subunits, although the role of D242 appears to be unique for KCNQ1.

Conclusions and Implications: Our findings reveal a new structural modality for ligand-induced activation of an important potassium channel, which can be harnessed for development of KCNQ-targeting pharmaceutics.

KEYWORDS

KCNQ/Kv7, phosphatidylinositol 4,5-bisphosphate, voltage-gated potassium channel, zinc

Abbreviations: cDNA, complementary DNA; DMEM, Dulbecco's modified Eagle's medium; HMR1556, N-[(3R,4S)-3,4-dihydro-3-hydroxy-2,2-dimethyl-6-(4,4,4-trifluorobutoxy)-2H-1-benzopyran-4-yl]-N-methylmetanesulfonamide; KCNE, Potassium voltage-gated channel subfamily E regulatory subunit; KCNQ, Potassium voltage-gated channel subfamily Q; ML277, (2R)-N-[4-(4-Methoxyphenyl)-2-thiazolyl]-1-[(4-methylphenyl)sulfonyl]-2-piperidinecarboxamide; PD, pore domain; PDTC, Pyrrolidinedithiocarbamate; RTG, Retigabine; TPEN, N,N,N′,N′-tetrakis-(2-Pyridylmethyl) ethylenediamine; VSD, Voltage-sensing domain; ZnPy, Zinc pyrithione.

1 | INTRODUCTION

The **KCNQ (Kv7)** family of voltage-gated K^+ channels encompasses five members (KCNQ1–5; Kv7.1–Kv7.5) with robust and well-studied functions in neurons, muscle cells, epithelia and several other cell and tissue types (Abbott, 2020; Barrese et al., 2018; Gamper & Shapiro, 2015; Jones et al., 2021). The family is unevenly split into predominantly neuronal KCNQ2–5, also called 'M-type' channels (Brown & Adams, 1980; Brown & Passmore, 2009) and predominantly non-neuronal KCNQ1 (previously known as KvLQT1), which is mostly expressed in the cardiovascular system and epithelia (Hamilton & Devor, 2012; Schreiber & Seebohm, 2021; Stott et al., 2014). While KCNQ2–5 form various heteromeric combinations, KCNQ1 does not seem to multimerise with any other KCNQ subunits but forms complexes with KCNE β-subunits (Abbott, 2021). KCNQ1 is expressed in the heart, airways, uterus, pancreas, gastrointestinal tract, kidneys and inner ear (Barhanin et al., 1996; Sanguinetti et al., 1996). In the heart, KCNQ1, in complex with KCNE1, forms a slow delayed-rectifier K^+ current, I_{Ks}, crucial for repolarisation of the cardiac action potential and setting the QT interval in the electrocardiogram (Barhanin et al., 1996; Nicolas et al., 2008; Sanguinetti et al., 1996). KCNQ/KCNE1 complexes are also found in the inner ear and in the pancreatic acinar cells (Kottgen et al., 1999; Robbins, 2001; van der Horst et al., 2020; Wang & Li, 2016). Accordingly, *KCNQ1* mutations often result in arrhythmias (long QT syndrome, LQTS), an inherited form of deafness (Kapplinger et al., 2015; Mousavi Nik et al., 2015; Oertli et al., 2021), as well as in impaired ß-cell function (Ullrich et al., 2005) with possible links to type 2 diabetes (Unoki et al., 2008; Zhang et al., 2020). In many epithelia and some other non-excitable cells, KCNQ1 co-assemble with KCNE3, forming a constitutively open channel (Abbott, 2021; Sun & MacKinnon, 2020) which contributes to water and salt transport (Schroeder et al., 2000; Vallon et al., 2005).

Being a key regulator of excitability and solute transport, KCNQ channel abundance and activity is tightly controlled via endogenous modulatory pathways, such as **G protein coupled receptor signalling** pathways, phosphorylation and other post-translational modifications, trafficking, transcriptional regulation, and so forth (reviewed in Delmas & Brown, 2005; Gamper & Shapiro, 2015; Greene & Hoshi, 2016; Jones et al., 2021). Likewise, an increasing number of natural and synthetic compounds were identified as KCNQ modulators, of which the majority are activators (Borgini et al., 2021; Du et al., 2018; Jones et al., 2021; Liu et al., 2021). The KCNQ channel activators or 'openers' are of particular therapeutic value because of their anti-excitatory action in the nervous system, supporting anticonvulsant and analgesic efficacy (Du et al., 2018; Jones et al., 2021; Liu et al., 2021; Perucca & Taglialatela, 2025). Intracellular free zinc was recently discovered as a potent activator of KCNQ channels (Gao et al., 2017; Yang et al., 2023). Zinc was suggested to potentiate channel activity by reducing or removing its dependency on the **phosphatidylinositol 4,5-bisphosphate (PIP_2)**, an obligatory cofactor necessary for KCNQ channel activity (Gao et al., 2017). Accordingly, all KCNQ isoforms, except KCNQ3 (Kv7.3), which has a very high PIP_2 affinity, are activated by zinc ionophores (Gao et al., 2017; Xiong et al., 2007; Yang et al., 2023).

What is already known?

- KCNQ (Kv7) channels are important regulators of excitability and epithelial transport.
- KCNQ channels are activated by intracellular zinc but its binding site is unknown.

What does this study add?

- A partially conserved zinc coordination site in KCNQ channels is identified.
- It is involved in voltage-sensing and PIP_2 interaction.

What is the clinical significance?

- This insight may help the design of KCNQ channel activators for treatment of excitability disorders.

Zinc is an essential trace metal, it is a necessary structural or catalytic cofactor for many transcription factors, enzymes and receptors; it is also increasingly recognised as a prominent intracellular and extracellular signalling molecule (Kambe et al., 2014). Zinc signalling is an important factor in the nervous (Blakemore & Trombley, 2017) and cardiovascular systems (Dorward et al., 2023). In the nervous system, zinc is stored in synaptic vesicles (particularly the glutamate-containing ones) and released in an activity-dependent manner, modulating a number of postsynaptic receptors (Takeda, 2014; Upmanyu et al., 2022). In the cardiovascular system, oxidative stress and acidification release zinc from its intracellular stores (Kambe et al., 2015), and such zinc signals were shown to affect ryanodine receptor-mediated calcium release and excitation–contraction coupling in the heart (Dorward et al., 2023; Reilly-O'Donnell et al., 2017; Turan et al., 1997). Thus, modulation of neuronal and cardiac KCNQ currents by zinc can have great implications for both nervous and cardiovascular systems. In addition, functional expression of KCNQ1 in skeletal muscle and epithelia may bestow further possibilities for physiological modulation of these channels by zinc.

Mechanistically, zinc-mediated KCNQ channel augmentation is mediated by reducing or even removing channel dependence on PIP_2 (Gao et al., 2017); however, the exact structural mechanism and zinc binding site(s) in KCNQ channels remain elusive, despite significant effort (Gao et al., 2017; Yang et al., 2023). Here we capitalised on a previous observation that binding of KCNE1 or KCNE3 subunits to KCNQ1 abolishes channel augmentation by a zinc ionophore (Gao et al., 2008). We hypothesised that the putative zinc

binding site in KCNQ1 could be obscured by KCNE binding, thus, narrowing the search area. Indeed, we identified what is likely to be a zinc coordination site of KCNQ1; it interacts with both the KCNE1/3- and PIP_2-binding areas of KCNQ1, which might explain previous observations. The site is partially conserved with KCNQ4, KCNQ2 and, likely, other KCNQ subunits. These findings reveal new regulation mode of an important potassium channel family.

2 | METHODS

2.1 | Cell culture and transfection

Chinese hamster ovary (CHO, KCB Cat#KCB83004YJ; RRID: CVCL_0213) and human embryonic kidney 293 (HEK293, KCB Cat#KCB200744YJ; RRID: CVCL_0063) cells were obtained from Kunming Institute of Zoology, Chinese Academy of Sciences. Cells were grown in T25 flasks in Dulbecco's modified Eagle's medium (DMEM) with 10% fetal bovine serum and 0.1% penicillin/streptomycin in a humidified incubator at 37°C (5% CO_2) and passaged about every 2 days. CHO cells were transfected with the following cDNA constructs: human *KCNQ2* (GeneBank accession no. Y15065), human *KCNQ4* (GeneBank accession no. AF105202), human *KCNQ1* (GeneBank accession no. NM000218), human *KCNE1* (GeneBank accession no. NM000219) and human *KCNE3* (GeneBank accession no. NM005472). cDNAs were subcloned into pCDNA3.1 (Youbio, Hunan, China). Point mutations in *KCNQ1*, *KCNQ2* and *KCNQ4* were produced by Youbio (Hunan, China). CHO cells were used for most studies; HEK293 cells were used in studies where double mutant cDNA constructs of *KCNQ1*, *KCNQ2* and *KCNQ4* were used. Both CHO and HEK293 cells were transfected with Lipo 8000 Transfection Reagent (Beyotime, China), according to the manufacturer's instructions; the experiments were performed 48 h after transfection. As a marker for successfully transfected cells, cDNA-encoding GFP was cotransfected together with the other genes of interest.

2.2 | Patch-clamp recording

The perforated patch configuration of the patch-clamp technique was used to voltage clamp and dialyse cells. Recordings were performed at room temperature (22–25°C) using amphotericin B (0.5 mg ml^{-1}) as a pore-forming agent. Pipettes were pulled from borosilicate glass capillaries using a Flaming/Brown micropipette puller P-97 and had resistances of 3 to 5 MΩ. Currents were amplified by the EPC10 USB amplifier (HEKA, Stuttgart, Germany) and recorded using the Patchmaster software (v2x90.4, 2018; HEKA, Studgart, Germany). Capacitance current artefacts were cancelled, and series resistance was compensated by 80%. To evaluate the amplitude of KCNQ1 and KCNQ1/KCNE1(3) currents (and those from relevant mutants), CHO cells were held at −80 mV, and 2000 ms depolarising steps to 30 mV, followed by a 500 ms pulse back to −50 mV, were applied every 2.7 s. The effects of the compounds on ion channel activity was evaluated by analysing steady-state currents at +30 mV. The effect of **Zinc pyrithione** (ZnPy) on KCNQ1(H126A/E170A) was estimated by assessing its effect on the HMR1556-sensitive fraction of the current. To evaluate the amplitude of currents conducted by KCNQ2, KCNQ4 and the relevant mutants, CHO cells were held at 0 mV and 1000 ms hyperpolarising steps to −60 mV, followed by a 500 ms pulse back to 0 mV, were applied every 1.7 s. The effects of the compounds on ion channel activity was evaluated by analysing steady-state currents at 0 mV. The activation curves were obtained by a series of voltage steps. To record the KCNQ1, KCNQ1(D242A), KCNQ1(D242A)/KCNE1 currents, CHO cells were held at −80 mV and stimulated by a series of 3000 ms depolarising steps from −70 to 50 mV in 10 mV increments. A testing step to −60 mV was applied to obtain tail currents. To record KCNQ1/KCNE1 currents, CHO cells were held at −80 mV and stimulated by a series of 3000 ms depolarising steps from −60 to 120 mV in 10 mV increments, and a − 60 mV testing step was used to obtain tail currents. Ion channel activity was evaluated by analysing steady-state currents at the end of each voltage pulse. G was calculated as the ratio of steady-state current amplitude to driving force ($G = I/(V - V_{rev})$. The data were fitted by the Boltzmann Sigmoidal equation: $G = G_{min} + (G_{max} - G_{min})/(1 + \exp[V - V_{1/2}]/S)$), where G_{max} is the maximum conductance, G_{min} is the minimum conductance, $V_{1/2}$ is the voltage for reaching 50% of maximum conductance, and S is the slope factor.

2.3 | Solutions and reagents

The external solution for patch-clamp recording from the CHO cells contained (in mM) 160 NaCl, 2.5 KCl, 2 $CaCl_2$, 1 $MgCl_2$ and 10 HEPES (pH adjusted to 7.4 with NaOH). The pipette solution for perforated patch contained (in mM) 90 K-acetate, 20 KCl, 1 $CaCl_2$, 3 $MgCl_2$, 10 HEPES, 3 ethylene glycol tetraacetic acid (EGTA), and 0.5 mg ml^{-1} amphotericin B (pH adjusted to 7.4 with KOH). The intracellular solution for experiments was prepared daily and filtered with 0.22 μm sterile microfilters. Reagents were obtained as follows: Zinc pyrithione (ZnPy), N,N,N′,N′-tetrakis-(2-Pyridylmethyl) ethylenediamine (TPEN), XE991, Retigabine (RTG), amphotericin B, $ZnCl_2$ and Pyrrolidine dithiocarbamate (PDTC) (Sigma-Aldrich, Darmstadt, Germany); (2R)-N-[4-(4-Methoxyphenyl)-2-thiazolyl]-1-[(4-methylphenyl)sulfonyl]-2-piperidinecarboxamide (ML277) and N-[(3R,4S)-3,4-Dihydro-3-hydroxy-2,2-dimethyl-6-(4,4,4-trifluorobutoxy)-2H-1-benzopyran-4-yl]-N-methylmetanesulfonamide (HMR1556) (MedChemExpress, Monmouth Junction, USA); and DMEM and fetal bovine serum (Gibco, Waltham, USA).

2.4 | Structural modelling

The cryo-EM structures of KCNQ1 (PDB ID: 6v01) (Sun & MacKinnon, 2020), KCNQ2 (PDB ID: 8j01) (Ma et al., 2023) and KCNQ4 (PDB ID: 7byl) (Li et al., 2021) were used for structural

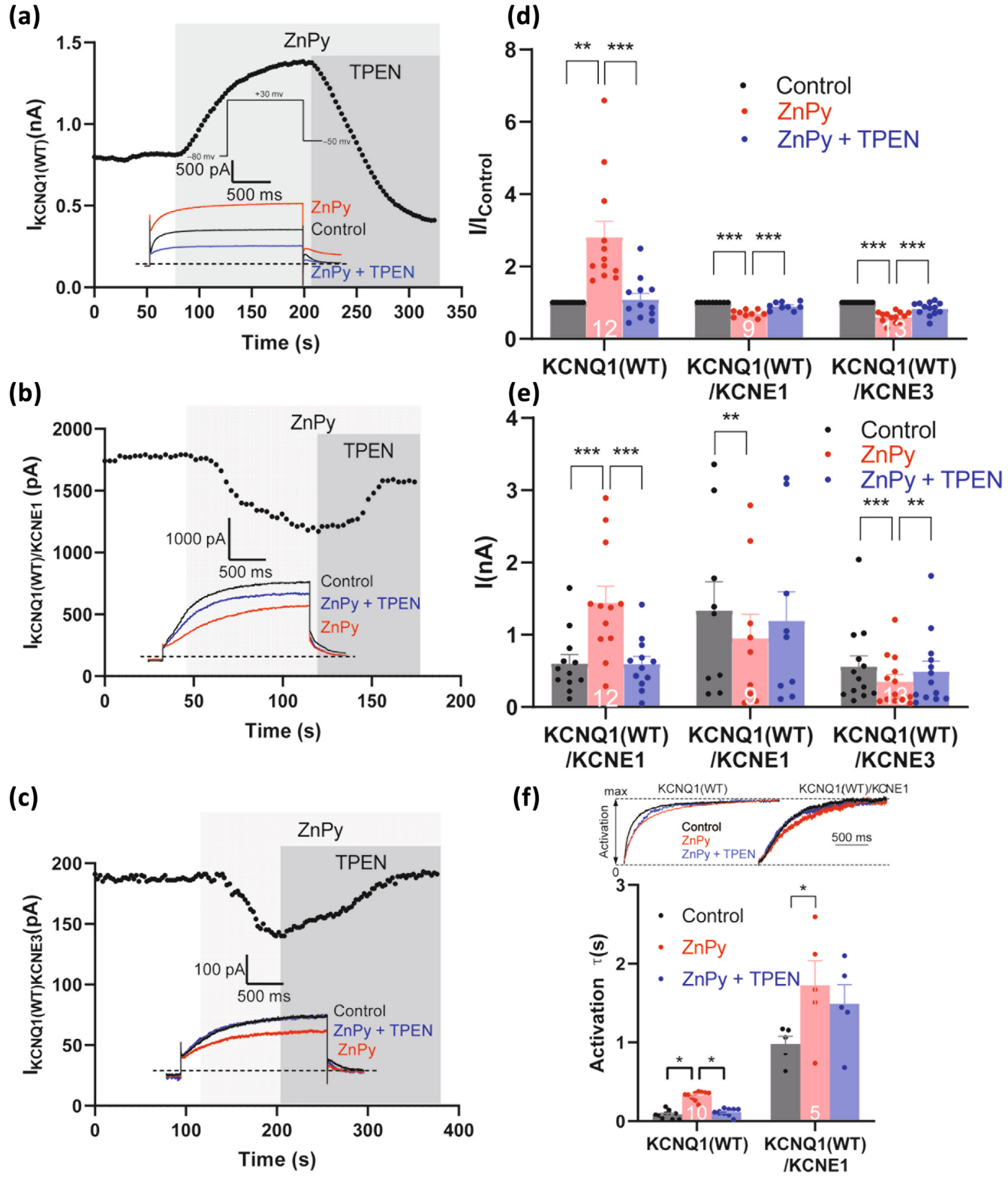

FIGURE 1 Legend on next page.

analysis. Zinc was manually inserted into the putative binding sites for visualisation purposes. Open-source PyMOL software was used to perform structural display, electrostatic analysis and histidine distribution analysis.

The Gaussian Network Model (GNM) was used to analyse the cross-correlation of residues between KCNE3 and KCNQ1. In brief, the Gaussian network model is based on considering the α-carbon atom of each residue of a protein as a node; the nodes are connected to each other by springs to form an elastic network. The global motion of the protein is captured by the simplified spring network, while the residue interrelationship diagram visualises the synergistic or antisynergistic motion patterns between residues. By analysing these patterns, functional conformational changes of a protein of interest can be inferred, providing clues for protein dynamics.

2.5 | Statistical analysis

The data and statistical analysis were conducted in accordance with the guidelines for experimental design and analysis in pharmacology as recommended by the *British Journal of Pharmacology* (Curtis et al., 2025). Electrophysiological recordings in transfected CHO and HEK293 cells were obtained from cells residing in separate cell culture dish or well, and independently transfected, hence, data obtained from each such dish/well represent an independent experiment. Statistical analysis was conducted exclusively for studies in which each group contained a minimum of five independent observations. The data were analysed and plotted with SPSS and GraphPad Prism 9.5 (GraphPad Software). All data are presented as mean ± SEM. Differences between groups were assessed by Student's *t*-test (paired or unpaired, as appropriate) or non-parametric Mann–Whitney tests (for the data that did not meet the normality and homogeneity of variance tests). One-way or repeated-measures analysis of variance (ANOVA), followed by Bonferroni's post hoc test, Dunnett's test, or Tukey's test, was performed for multiple group comparison, depending on the specific requirements of the analysis. Post hoc tests were only performed if the *F*-value was significant ($P < 0.05$) and there was no significant heterogeneity of variance. The differences were considered significant at $P < 0.05$.

2.6 | Nomenclature of targets and ligands

Key protein targets and ligands in this article are hyperlinked to corresponding entries in the IUPHAR/BPS Guide to PHARMACOLOGY http://www.guidetopharmacology.org and are permanently archived in the Concise Guide to PHARMACOLOGY 2023/2024 (Alexander, Christopoulos et al., 2023; Alexander, Fabbro et al., 2023; Alexander, Mathie et al., 2023).

3 | RESULTS

3.1 | Binding of KCNE1 or KCNE3 subunits to KCNQ1 abolishes zinc-mediated channel activation

We first investigated the effect of auxiliary subunits KCNE1 and KCNE3 on the ability of zinc ionophores to activate KCNQ1. Consistent with previous findings (Gao et al., 2017; Z. Gao et al., 2008; Xiong et al., 2007), KCNQ1 homomers transiently overexpressed in CHO cells were potently activated by ZnPy (10 μM; Figure 1a,d,e) and PDTC (20 μM; Figure S1a,d,e). These compounds are zinc ionophores, molecules that promote intracellular zinc accumulation (Scavo & Oliveri, 2022). Thus, ZnPy increased steady-state current amplitude at a saturating voltage of +30 mV by 2.81 ± 0.42 fold ($n = 12$, $P < 0.01$) and PDTC similarly produced an increase by 2.67 ± 0.53 fold ($n = 7$, $P < 0.05$). The augmentation was completely reverted by a zinc chelator, TPEN (20 μM), applied still in the presence of ionophore, confirming that the active component is zinc, not the ionophore. Co-expression of KCNQ1 with either KCNE1 (Figures 1b,d,e and S1b,d,e) or KCNE3 (Figures 1c,d,e and S1c,d,e) not only abolished zinc ionophore-induced augmentation but resulted in a significant inhibition of the heteromeric channels instead; this effect was also reversed by TPEN (Figure 1d,e). These results elucidated that in the presence of KCNE subunits, the primary activating effect of zinc is abolished and a secondary inhibitory action (perhaps a pore block) is revealed. Indeed, consistent with previous finding (Gao et al., 2017), application of extracellular $ZnCl_2$ (50 μM) in the absence of an ionophore induced small but measurable inhibition of both the KCNQ1homo-tetramer and the KCNQ1/KCNE1 complex (Figure S2).

FIGURE 1 **Auxiliary KCNE1 and KCNE3 subunits abolish zinc-mediated activation of KCNQ1.** (a) Perforated patch-clamp recording from a Chinese hamster ovary (CHO) cell transfected with *KCNQ1*; shown is the time course for the effects of the Zn^{2+} ionophore, zinc pyrithione (ZnPy; 10 μM) and the Zn^{2+} chelator, N,N,N′,N′-tetrakis-(2-Pyridylmethyl) ethylenediamine (TPEN, 20 μM), as labelled. Example current traces and the voltage protocol are shown in the inset underneath. Vertical grey bars indicate periods of drug application. (b) CHO cells were co-transfected with *KCNQ1* and *KCNE1*; recording conditions and labelling are similar to that used in Figure 1a. (c) CHO cells were co-transfected with *KCNQ1* and *KCNE3*; recording conditions and labelling are similar to that used in Figure 1a,b. (d and e) Summary of the experiments shown in Figure 1a–c. Normalised current amplitudes (relative to basal amplitude, $I_{control}$) are summarised in Figure 1d, and mean current amplitudes are summarised in Figure 1e; number of experiments is indicated within the bars. Asterisks depict significant difference between the groups indicated by connector lines; $^{*}P < 0.05$, $^{**}p < 0.01$; $^{***}P < 0.001$ (repeated-measures ANOVA with Bonferroni post hoc test). (f) Summary of the effects of the ZnPy and TPEN on the activation time constant (τ) at +30 mV voltages; τs were obtained by fitting the activation traces with an exponential function. Example current traces shown above the bar charts are scaled up to maximal amplitude. Asterisks depict significant difference from control; $^{*}P < 0.05$ (repeated-measures ANOVA with Bonferroni post hoc test).

TABLE 1 Effects of intracellular Zn^{2+} on the KCNQ1 channel current amplitude and activation kinetics.

	Steady-state current amplitude (30 mV)			Activation τ (ms)			$V_{1/2}$	
Channel variant	**Control**	**ZnPy**	**ZnPy + TPEN**	**Control**	**ZnPy**	**ZnPy + TPEN**	**Control**	**ZnPy**
KCNQ1 WT	606.4 ± 123.0 $n = 12$	1445.7 ± 225.6 $n = 12$	596.9 ± 104.9 $n = 12$	86.1 ± 16.0 $n = 10$	327.2 ± 17.2 $n = 10$	115.9 ± 13.8 $n = 10$	−9.7 ± 3.3 $n = 6$	−10.2 ± 5.8 $n = 6$
KCNQ1 WT + KCNE1	1330.3 ± 400.0 $n = 9$	976.3 ± 324.0 $n = 9$	1215.1 ± 393.9 $n = 9$	978.2 ± 101.6 $n = 5$	1726.5 ± 311.8 $n = 5$	1491.9 ± 241.5 $n = 5$	64.5 ± 3.2 $n = 5$	73.2 ± 5.1 $n = 5$
KCNQ1 WT + KCNE3	560.07 ± 149.8 $n = 13$	354.85 ± 96.08 $n = 13$	496.45 ± 139 $n = 13$	701.3 ± 151.4 $n = 5$	1063.5 ± 197.4 $n = 5$	627.3 ± 104.5 $n = 5$		
KCNQ1 D242A	697.4 ± 170.7 $n = 7$	412.9 ± 98.3 $n = 7$		145.9 ± 18.5 $n = 7$	76.0 ± 14.5 $n = 7$		−39.4 ± 1.9 $n = 5$	
KCNQ1 D242A + KCNE1	224 ± 78.7 $n = 6$	395.3 ± 124.2 $n = 6$	258.5 ± 81.0 $n = 6$	372.9 ± 84.5 $n = 6$	201.1 ± 24.2 $n = 6$	341.7 ± 71.3 $n = 6$	−21.8 ± 8.3 $n = 5$	
KCNQ1 D242A + KCNE3	91.6 ± 18.2 $n = 5$	279.2 ± 94.5 $n = 5$		547.4 ± 110.0 $n = 4$	158.3 ± 29.3 $n = 4$			
KCNQ1 D242K	559 ± 157.4 $n = 6$	640.8 ± 170.2 $n = 6$		281.2 ± 16.8 $n = 6$	244.2 ± 24.2 $n = 6$			
KCNQ1 D242E	186.9 ± 41.0 $n = 6$	395.2 ± 101.8 $n = 6$		376.1 ± 31.8 $n = 5$	283.2 ± 54.2 $n = 5$			
KCNQ1 H126A	105.9 ± 19.6 $n = 10$	153.7 ± 24.4 $n = 10$	80.3 ± 19.9 $n = 10$					
KCNQ1 H240A	170.9 ± 39.3 $n = 8$	359.6 ± 60.9 $n = 8$	176.2 ± 40.1 $n = 8$					
KCNQ1 E170A	113.4 ± 16.1 $n = 8$	196.2 ± 29.5 $n = 8$	95.0 ± 16.6 $n = 8$					
KCNQ1 H126A/E170A	296.7 ± 55.2 $n = 13$	338.1 ± 58.4 $n = 13$	258.9 ± 57.4 $n = 13$					
KCNQ1 H126A/E170A + KCNE1	74.6 ± 18.3 $n = 10$	70.37 ± 16.9 $n = 10$						
KCNQ1 H126A/H240A/E170A	35.3 ± 6.1 $n = 8$	36.4 ± 7.2 $n = 8$						
KCNQ1 H126A/H240A/E170A + KCNE1	38.8 ± 11.5 $n = 9$	40.8 ± 12.4 $n = 9$						

In addition to a marked increase in KCNQ1 current amplitude, ZnPy treatment also slowed channel activation kinetics at saturating voltages (Figure 1f and Table 1). This effect was also reverted by TPEN. In the presence of KCNE1 or KCNE3, the KCNQ1/KCNE1 became much slower (Figures 1 and S1; Table 1), as expected (Abbott, 2021). Interestingly, ZnPy still produced further slowing of the KCNQ1/KCNE1 and KCNQ1/KCNE3 heteromeric currents (Figure 1f and Table 1), suggesting that this effect could be associated with the secondary action of zinc.

The currents generated by KCNQ1/KCNE3 complexes were generally described as voltage-independent or 'instantaneous' (Bendahhou et al., 2005; Schroeder et al., 2000). In our recordings, KCNQ1/KCNE3, while having an instantaneous component, also had a slow-kinetic voltage-dependent current component (e.g. Figures 1c and 3c). The reasons could be either a presence of KCNQ1 homotetramers or some endogenous factors present in the expression system. Nevertheless, clear abolition of zinc-mediated potentiation of macroscopic current by KCNE3 does suggest that the majority of channels in these recordings were indeed KCNQ1/KCNE3 multimers.

3.2 | Elucidating zinc binding site of KCNQ1

Zinc binding sites in proteins are often complex and contain histidine or cysteine residues, as well as aspartic or glutamic acids (Alberts et al., 1998; Vallee & Falchuk, 1993). Previously, in search for zinc binding site responsible for activation of KCNQ4 channel, we performed alanine substitutions of all intracellularly facing histidines (one by one), as well as all intracellular cysteines conserved between KCNQ2–4 (Gao et al., 2017). None of these substitutions abolished channel activation by zinc. Additionally, a KCNQ4 channel with a histidine-less C terminus, H(330, 334, 569, 669)A, and a triple-cysteine substitution at positions C(156–158)A of the S2–S3 linker were also still fully sensitive to zinc activation (Gao et al., 2017). These earlier experiments revealed that zinc binding site in the KCNQ channels is likely to be complex.

In search for additional hints, we reasoned that because binding of the KCNE subunits abolishes zinc-mediated KCNQ1 current augmentation, zinc binding site on KCNQ1 could reside within the KCNQ1/KCNE interface. We analysed the available KCNQ1/KCNE3/Calmodulin structure (6v01; Sun & MacKinnon, 2020) and focussed on the groove occupied by the KCNE3 (Figure 2a,b). We analysed the distribution of histidines in the KCNQ1 structure (Figure 2a, left panel) and noticed a site containing two histidines in close proximity (H126, H240) and the acidic residue, E170. Additionally, D242 of the S4–S5 linker is located nearby, and it is coupled with H240. The pocket features a mixture of histidines and negatively charged residues (glutamic and aspartic acids) often seen in zinc coordination sites of proteins (Alberts et al., 1998; Vallee & Falchuk, 1993). This site nears the region of the voltage-sensing domain (VSD) and partly interacts with KCNE3 (Figure 2a,b). Importantly, this pocket may also interact with PIP_2 (Figure 2b), making it an interesting candidate site for mediating the channel 'opener' effect of zinc, which is affected by both KCNE (Figures 1 and S1) and PIP_2 (Gao et al., 2017). Analysis of the KCNQ1/KCNE3 structure shows that the H126, E170, and H240 side chains can coordinate Zn^{2+} positioned at this site (Figure 2a, centre and right panels). We further hypothesised that Zn^{2+} binding transmits the conformational signal from the S4–S5 linker to the pore domain (PD; S5–S6) to cause gating changes.

To explore this site, we first made a series of D242 substitutions. Substitution by hydrophobic alanine (D242A) completely abolished ZnPy-mediated KCNQ1 current augmentation, revealing (as in the case of KCNQ1/KCNE1 or KCNQ1/KCNE3 heteromers) a partially inhibitory effect instead (Figure 2c,d and Table 1). D242A substitution had a strong effect on KCNQ1 voltage-dependence and the biophysical outcomes of KCNQ1/KCNE1 interactions: the mutation shifted KCNQ1 voltage dependence by some −30 mV and strongly reduced positive shift induced by KCNE1 binding (Figure S3 and Table 1). These findings indicate that D242 is important for KCNQ1 voltage dependence and KCNQ1/KCNE1 interaction.

In contrast, charge-preserving substitution D242E resulted in a channel that is still activated by ZnPy (Figure 2e and Table 1), while inverting the charge with lysine (D242K) produced a channel which was largely insensitive to ZnPy (Figure 2f and Table 1). From these initial experiments, it appeared that D242 is indeed a key residue in zinc-mediated KCNQ1 augmentation, but is it a bona fide zinc binding site?

Strikingly, when a KCNQ1(D242A) mutant was co-assembled with either KCNE1 (Figure 3a,b,e) or KCNE3 (Figure 3c,d,f), such heteromeric channels fully regained their ability to be activated by intracellular zinc: ZnPy activated these channels by twofold or threefold and TPEN removed the activation. Instead of slowing the activation, which was seen with the wild-type (WT) KCNQ1, ZnPy treatment accelerated activation kinetics of the D242A mutant (Figure 3g and Table 1).

Keeping in mind that neither KCNQ1(D242A) homomeric channels nor WT KCNQ1/KCNE1(3) channels can be activated by zinc; this surprise finding suggested the following possible explanations: (i) insertion of KCNE1 or KCNE3 into WT KCNQ1 interferes with coupling of zinc binding to channel activation in WT KCNQ1; (ii) D242 may not participate in zinc binding directly but rather be involved in coupling of zinc binding to channel activation. (iii) The addition of a KCNE subunit somehow circumvents the loss of coupling between the 'true' zinc binding site and channel activation. (iv) When zinc activation is prevented, a secondary effect – partial inhibition is revealed.

In the next series of experiments, we mutated H126, H240 and E170 of KCNQ1, either alone or in combination. Neither of the single mutations (H126A, H240A and E170A) abolished zinc-mediated augmentation completely (Figure 4a–f; and Table 1). However, the ZnPy-induced fold-change of current amplitude was significantly reduced in H126A and E170A mutants, as compared to the WT KCNQ1 (Figure 4f and Table 1). Thus, ZnPy increased the WT KCNQ1 current by 2.81 ± 0.42 fold ($n = 12$), while for H126A and E170A mutants,

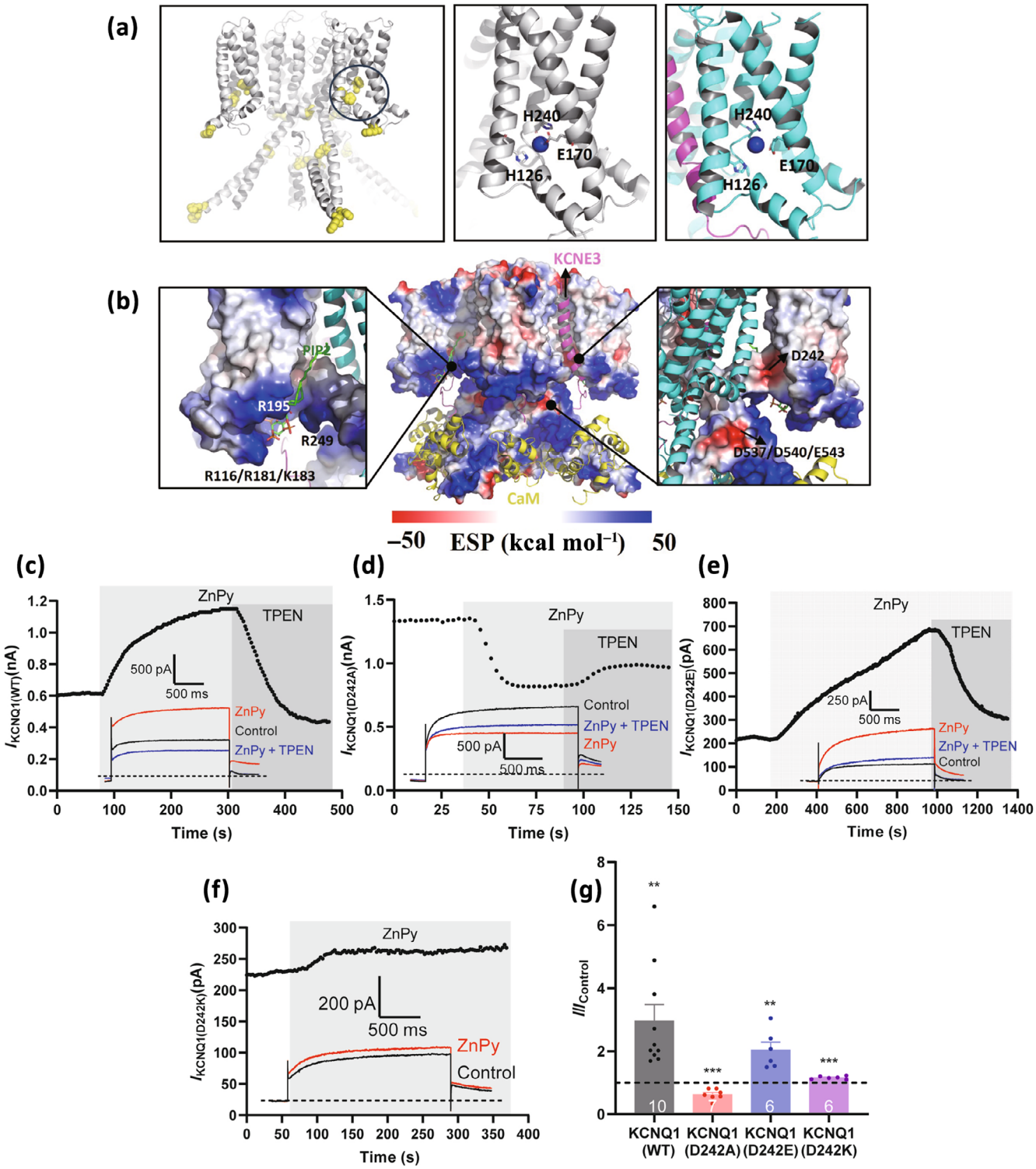

FIGURE 2 **D242 is important for zinc-mediated activation of KCNQ1.** (a) Histidine distribution map in the structure of KCNQ1 (left) and the putative zinc coordination site without (middle) or with (right) the presence of KCNE3 (shown in purple). (b) KCNQ1 electrostatic surface potential. Inset on the left depicts the PIP_2-binding pocket and inset on the right depicts the putative zinc-binding site. Modelling in Figure 2a,b is based on PDB ID: 6v01. (c–f) Perforated patch-clamp recordings from CHO cells transfected with *KCNQ1* (WT) (c), *KCNQ1*(D242A) (d), *KCNQ1* (D242E) (e), or *KCNQ1*(D242K) (f) showing the time courses for the effects of ZnPy (10 μM) and TPEN (20 μM), as indicated with vertical grey bars. Recording conditions and labelling are similar to that used in Figure 1a. (g) Summary of the experiments shown in Figure 2c–f. Normalised current amplitudes (relative to $I_{Control}$) are shown; number of experiments is indicated within the bars. Asterisks depict significant difference between the groups indicated by connector lines; $^{**}P < 0.01$ and $^{***}P < 0.001$ (paired Student's *t*-test or Wilcoxon signed-rank test for data that did not meet the normality and homogeneity of variance tests).

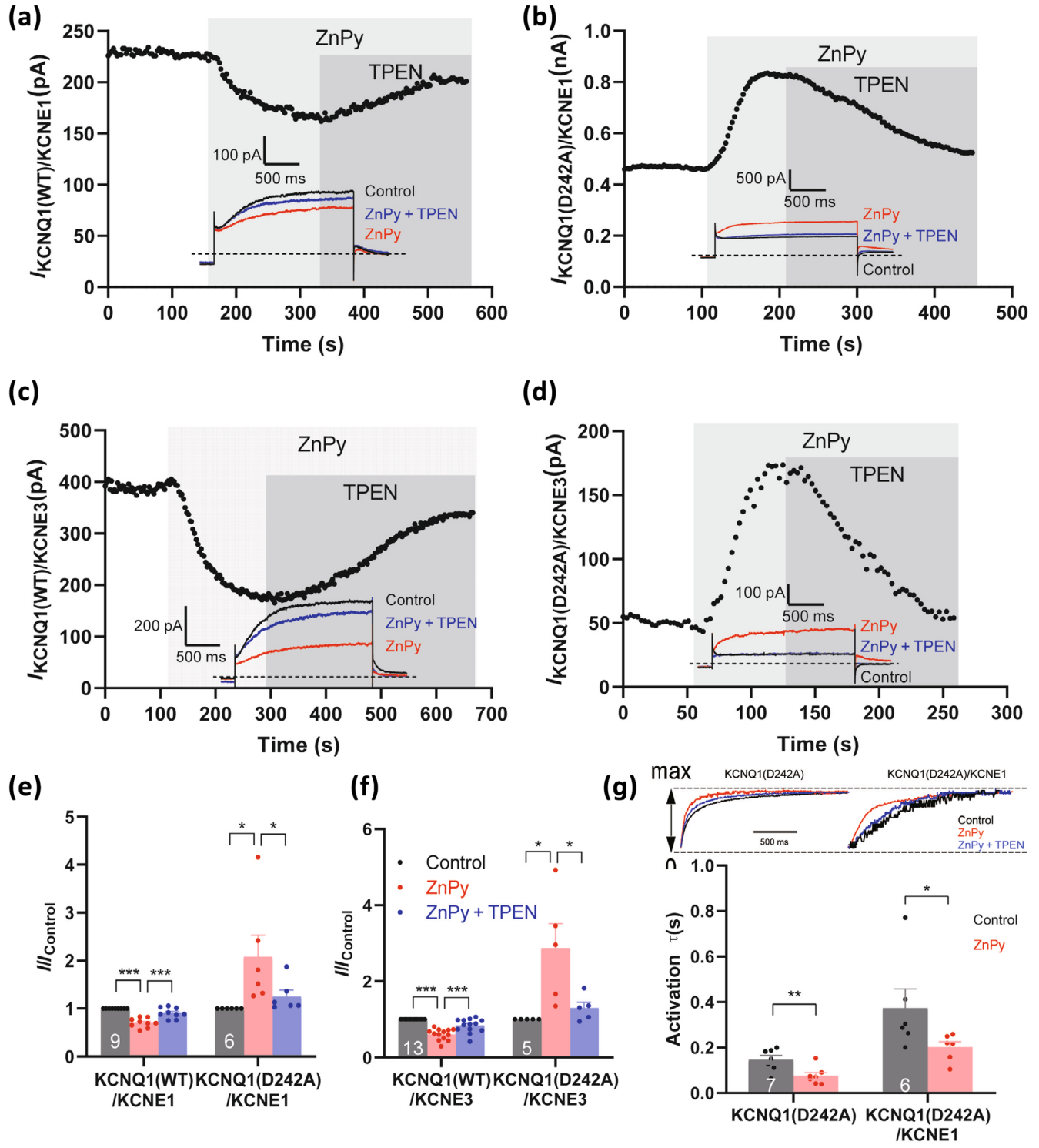

FIGURE 3 **KCNE1 or KCNE3 binding to KCNQ1 restores zinc sensitivity to the KCNQ1(D242A) mutant.** (a–d) Perforated patch-clamp recording from CHO cells co-transfected with *KCNQ1*(WT)/*KCNE1* (a), *KCNQ1*(D242A)/*KCNE1* (b), *KCNQ1*(WT)/*KCNE3* (c) and *KCNQ1*(D242A)/*KCNE3* (d); shown are the time courses of the effects of ZnPy (10 μM) and TPEN (20 μM). Recording conditions and labelling are similar to that used for Figure 1a. (e and f) Summary of experiments shown in Figure 3a–d. Normalised current amplitudes (relative to $I_{control}$) are shown; number of experiments is indicated within the bars. Asterisks depict significant difference between the groups indicated by connector lines; $^{*}P < 0.05$ and $^{***}P < 0.001$ (repeated-measures ANOVA with Bonferroni post hoc test). (g) Summary of the effects on the activation time constant (τ) at +30 mV voltages; τs were obtained by fitting the traces with an exponential function. Example current traces shown above the bar charts are scaled up to maximal amplitude. Asterisks depict a significant difference from control; $^{*}P < 0.05$ and $^{**}P < 0.01$ (paired Student's *t*-test or Mann–Whitney test for the data that did not meet the normality and homogeneity of variance tests).

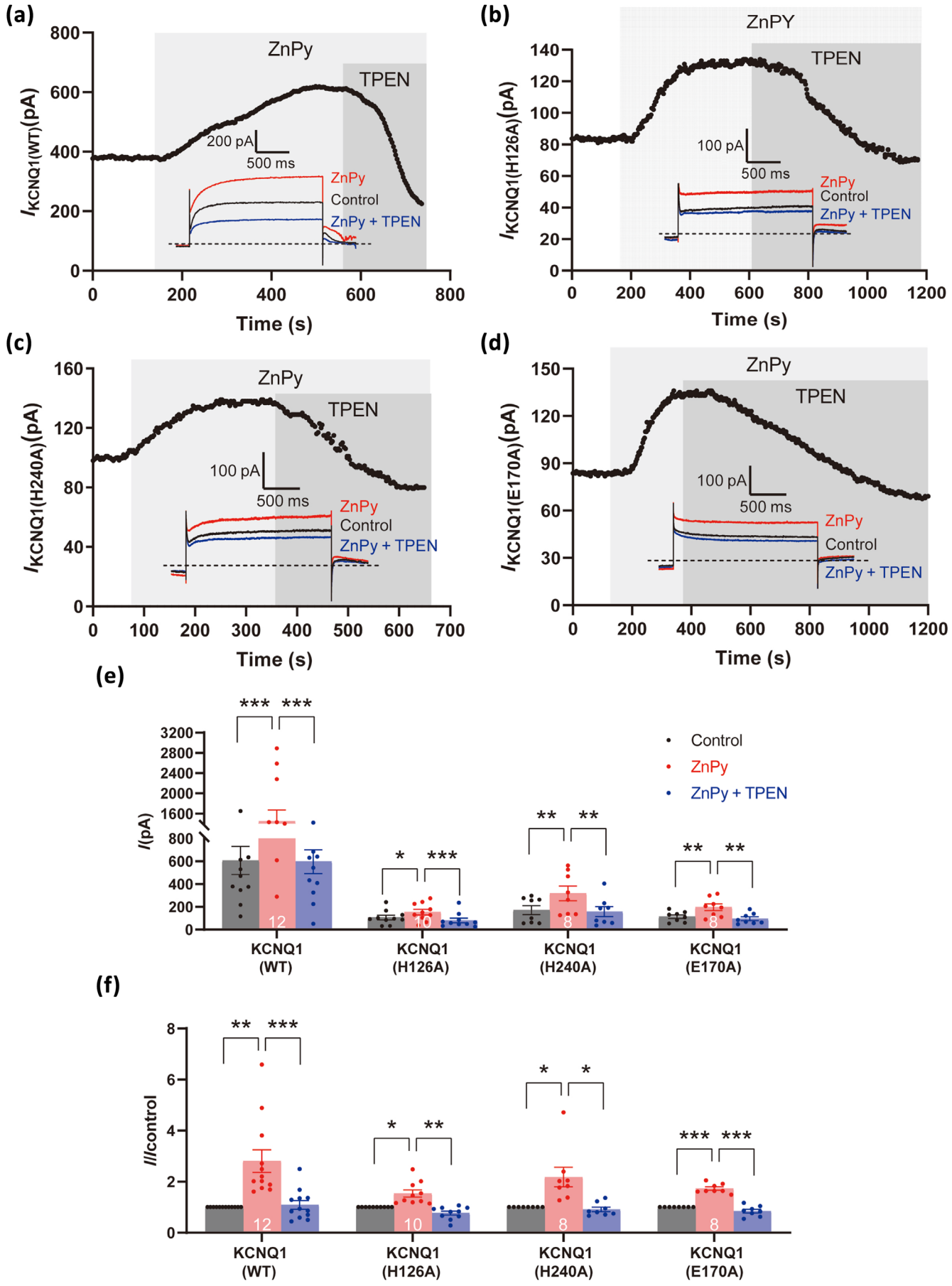

FIGURE 4 Legend on next page.

these values were 1.54 ± 0.14 fold ($n = 10$; $P < 0.05$) and 1.73 ± 0.07 fold ($n = 8$; $P < 0.05$), respectively. The ZnPy effect on H240A was somewhat reduced (2.18 ± 0.39 fold; $n = 8$) but not significantly different ($P = 0.28$) from that of the WT KCNQ1 (Figure 4f).

The double mutant, KCNQ1(H126A/E170A), produced very small currents in CHO cells but expressed better in HEK293 cells, where a significant current fraction sensitive to a selective KCNQ1/I_{Ks} inhibitor, HMR1556 (1 μM) (Thomas et al., 2003), was recorded (Figure 5a, d). This mutant was only mildly activated by ZnPy, showing a 1.52 ± 0.10 fold increase of the HMR1556-sensitive current fraction ($n = 12$; cf. 2.81 ± 0.42 fold increase seen in WT KCNQ1, $P < 0.001$; Figure 5a–c). Importantly, unlike in the case of D242A, co-assembly of KCNQ1(H126A/E170A) with KCNE1 did not restore activation by ZnPy (Figure 5d–f).

The triple mutant, KCNQ1(H126A/E170A/H240A), produced very small outward currents, which however were readily activated by the selective KCNQ1 channel opener, ML277 (1 μM) (Mattmann et al., 2012), and inhibited by HMR1556 (1 μM) (Figure S4a), suggesting that this mutant can still assemble as a functional channel. Remarkably, the triple mutant was entirely insensitive to ZnPy (Figure S4a–c).

In combination, these results suggest that H126A, E170A and H240A are important for zinc binding and coordination, and for KCNQ1 channel activation. This zinc coordination site can retain partial functionality even when either one of these residues is lost, but removal of two or three of the key residues results in nearly complete loss of zinc binding.

Application of the Gaussian Network Model (GNM) analysis of the KCNQ1 and KCNQ1/KCNE3 structures suggested that KCNE3 enhances the interaction between VSD and PD, as observed in the cross-correlation matrix plot (Figure S5). Based on this, and our functional and mutagenesis data, we hypothesise that D242 serves as a critical amino acid bridging the zinc-binding site and the pore domain of KCNQ1. Upon mutation to alanine, this bridging effect is lost, leading to the loss of the zinc-mediated activation. The addition of KCNE3 establishes a new connection with the VSD and PD, which helps restore the linkage between the zinc binding site (i.e. H240) and the pore-forming region (S5–S6). In contrast to the D242A mutation, zinc sensitivity of H126A/E170A or H126A/E170A/H240A mutants is not restored by KCNE1, suggesting that this may indeed be the true zinc coordination site of KCNQ1, while D242 serves as a bridge coupling zinc binding to pore opening. Hence, KCNE subunits may restore coupling of the zinc coordination site to the pore domain, which is lost in D242A mutant.

3.3 | Is zinc binding conserved amongst the KCNQ channel family?

We next asked if the zinc coordination site of KCNQ1 is conserved amongst other KCNQ channels. First, we mutated aspartic acids at the positions homologous to D242 of KCNQ1 in KCNQ2 and KCNQ4 channels (Figure S6a). Unlike KCNQ1(D242A), KCNQ2 (D212A) and KCNQ4(D218A) both displayed robust zinc-induced activation (Figure 6). ZnPy-induced fold-increase of current amplitude was even greater in KCNQ2(D212A), as compared to the WT KCNQ2 (Figure 6a,b,f). Such enhanced efficacy of zinc was previously seen in mutants with reduced PIP_2 affinity (Gao et al., 2017), which could be the case here as well, but we did not investigate this matter further. What was obvious is that the aspartic acid at the position homologous to D242 in KCNQ1 is not critical for zinc sensitivity of KCNQ2 and KCNQ4. This deviation may arise from the shorter S4–S5 linkers of KCNQ2 and KCNQ4, as compared to KCNQ1 (Figure 6e).

Next, we made two double mutants: KCNQ2(H96A/E140A) and KCNQ4 (H102A/E146A), at the positions equivalent to H126 and E170 of KCNQ1 (Figure S6a). Both mutants retained only minimal activation by ZnPy (Figure 7a–f). Thus, the current of WT KCNQ2 was activated by ZnPy by 1.41 ± 0.04 fold; $n = 14$; while for KCNQ2(H96A/E140A), the current was only increased by 1.09 ± 0.06 fold; $n = 6$, a significantly smaller increase ($P < 0.001$). Similarly, the current of WT KCNQ4 was activated by ZnPy by 3.15 ± 0.42 fold; $n = 10$; while for KCNQ4 (H102A/E146A), the current was increased by 1.28 ± 0.08 fold; $n = 11$, a significantly smaller effect ($P < 0.01$).

Finally, a triple KCNQ4 mutant with residues homologous to H126A, E170A and H240A of KCNQ1 was generated. This mutant produced very small currents but was still activated by the KCNQ-selective opener, RTG (20 μM), and inhibited by the KCNQ-selective inhibitor, XE991 (10 μM; Figure S6b–e), indicating that the mutant is still capable of assembly into a functional KCNQ channel. Notably, this mutant was completely insensitive to ZnPy (Figure S6b,c).

Together, our data suggest that the zinc binding site in KCNQ channels is partially conserved; residues homologous to KCNQ1 positions H126A, E170A and H240A are the core Zn^{2+} coordination residues (Figure 8a,b). There are some differences though; thus, D242 of the S4–S5 linker is uniquely important for coupling zinc binding to the channel gating in KCNQ1 but not in other KCNQ channels, perhaps because of the structural difference between the

FIGURE 4 **Elucidation of the zinc coordination site in KCNQ1.** (a–d) Perforated patch-clamp recordings from CHO cells transfected with *KCNQ1*(WT) (a), *KCNQ1*(H126A) (b), *KCNQ1*(H240A) (c), *KCNQ1*(E170A) (d); time courses of the effects of ZnPy (10 μM) and TPEN (20 μM) are shown. Recording conditions and labelling are similar to that used for Figure 1a. (e and f) Summary of experiments shown in Figure 4a–d, number of experiments is indicated within the bars. Mean current amplitudes are summarised in Figure 4e, and normalised current amplitudes (relative to basal amplitude, $I_{control}$) are summarised in Figure 4f. Asterisks depict significant difference between the groups indicated by connector lines; $^*P < 0.05$, $^{**}P < 0.01$ and $^{***}P < 0.001$ (repeated-measures ANOVA with Bonferroni post hoc test).

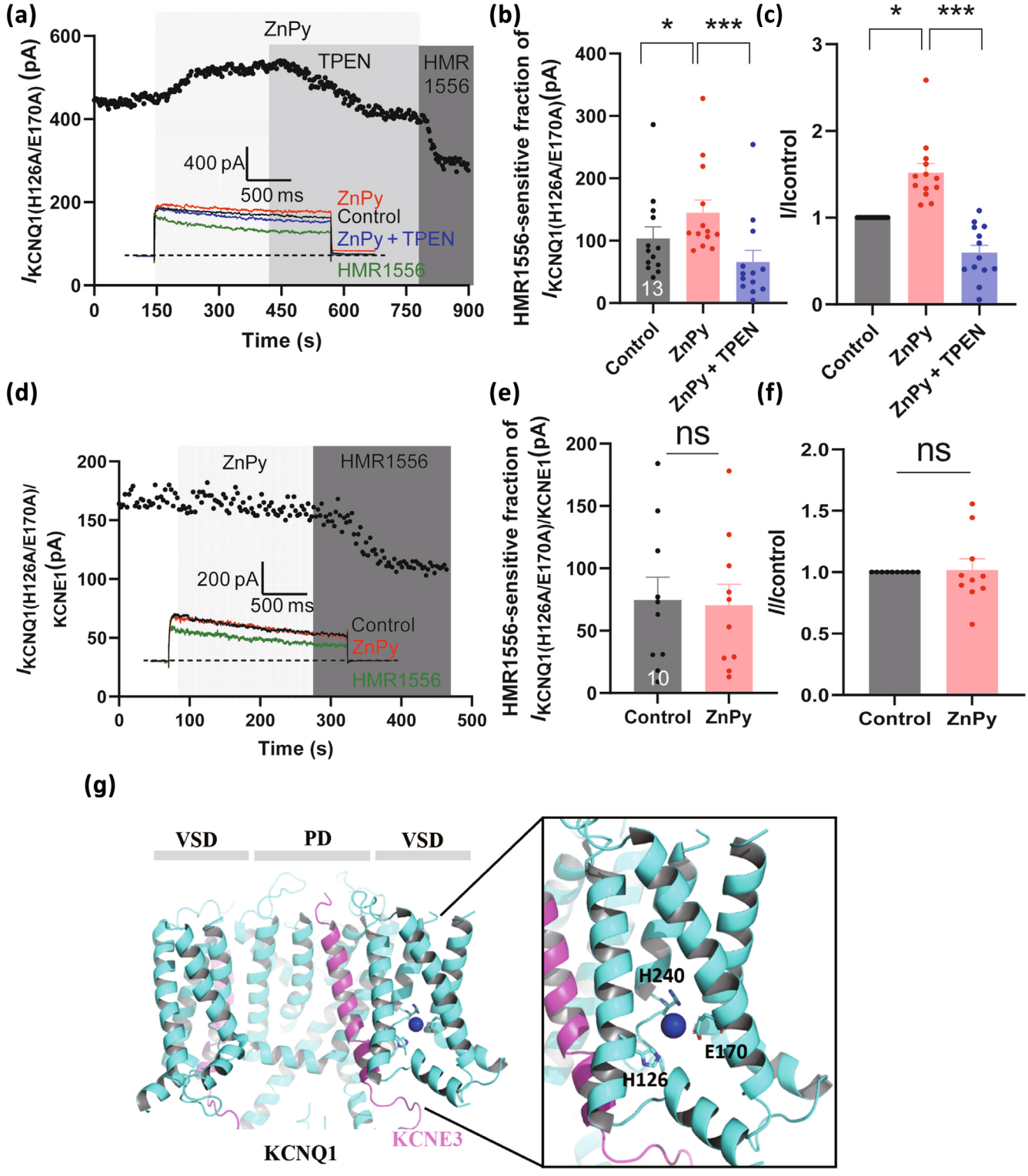

FIGURE 5 **Elucidation of the zinc coordination site in KCNQ1 – further insights.** (a–f) Perforated patch-clamp recording from HEK293 cells transfected with *KCNQ1*(H126A/E170A) (a–c) or *KCNQ1*(H126A/E170A)/*KCNE1* (d–f). Figure 5a,d shows the time courses of the effects of ZnPy (10 μM), TPEN (20 μM) (Figure 5a only) and HMR1556 (1 μM). Figure 5b,c,e,f shows summaries of experiments shown in Figure 5a,d; HMR1556-sensitive current fractions were analysed. Number of experiments is indicated within the bars. Mean current amplitudes are summarised in Figure 5b,e, and normalised current amplitudes (relative to basal amplitude, $I_{control}$) are summarised in Figure 5c,f. Asterisks depict significant difference between the groups indicated by connector lines; $^{*}P < 0.05$ and $^{***}P < 0.001$ (repeated-measures ANOVA with Bonferroni post hoc test or paired Student's *t*-test); ns, non-significant. (g) Structural depiction of the putative zinc coordination site within the KCNQ1/KCNE3 structure (PDB ID: 6v01). PD, pore domain; ns, non-significant; VSD, Voltage-sensing domain.

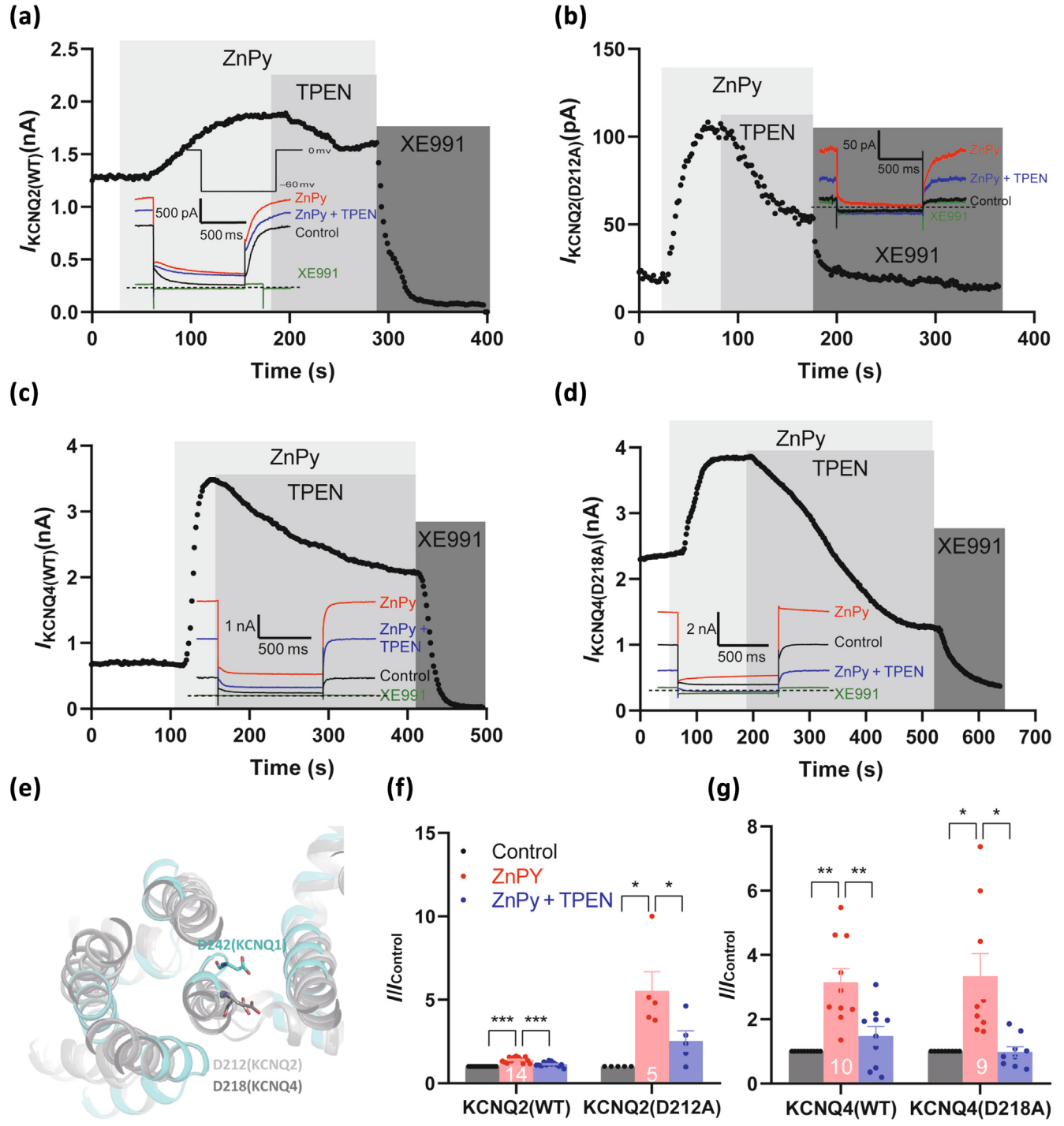

FIGURE 6 **Zinc sensitivity of KCNQ2 and KCNQ4 is not affected by the mutations equivalent to D242A in KCNQ1.** (a–d) Perforated patch-clamp recordings from CHO cells transfected with *KCNQ2* (WT) (a), *KCNQ2*(D212A) (b), *KCNQ4* (WT) (c) or *KCNQ4*(D218A) (d) showing the time courses for the effects of ZnPy (10 μM), TPEN (20 μM) and a KCNQ channel inhibitor, XE991 (10 μM), as indicated with vertical grey bars. (e) Alignment of the KCNQ1 (PDB ID: 7XNI), KCNQ2 (PDB ID: 7CR3) and KCNQ4 (PDB ID: 7BYL) structures revealed a longer S4–S5 linker in KCNQ1, as compared to KCNQ2 and KCNQ4. (f and g) Summary of the experiments shown in Figure 6a–d, number of experiments is indicated within the bars. Normalised current amplitudes (relative to basal amplitude, $I_{control}$) are summarised in Figure 6f,g. Asterisks depict a significant difference between the groups indicated by connector lines; $^{*}P < 0.05$, $^{**}P < 0.01$ and $^{***}P < 0.001$ (repeated-measures ANOVA with Bonferroni post hoc test).

KCNQ1 and other KCNQ subunits in this region (Figure 6e). Furthermore, the PIP_2 binding site in KCNQ2/4 is on the left side of the VSD, while in KCNQ1 is on the right side (Figure 8c). These differences may explain distinct electrophysiological outcomes of isoform-specific substitutions at the position homologous to D242 in KCNQ1.

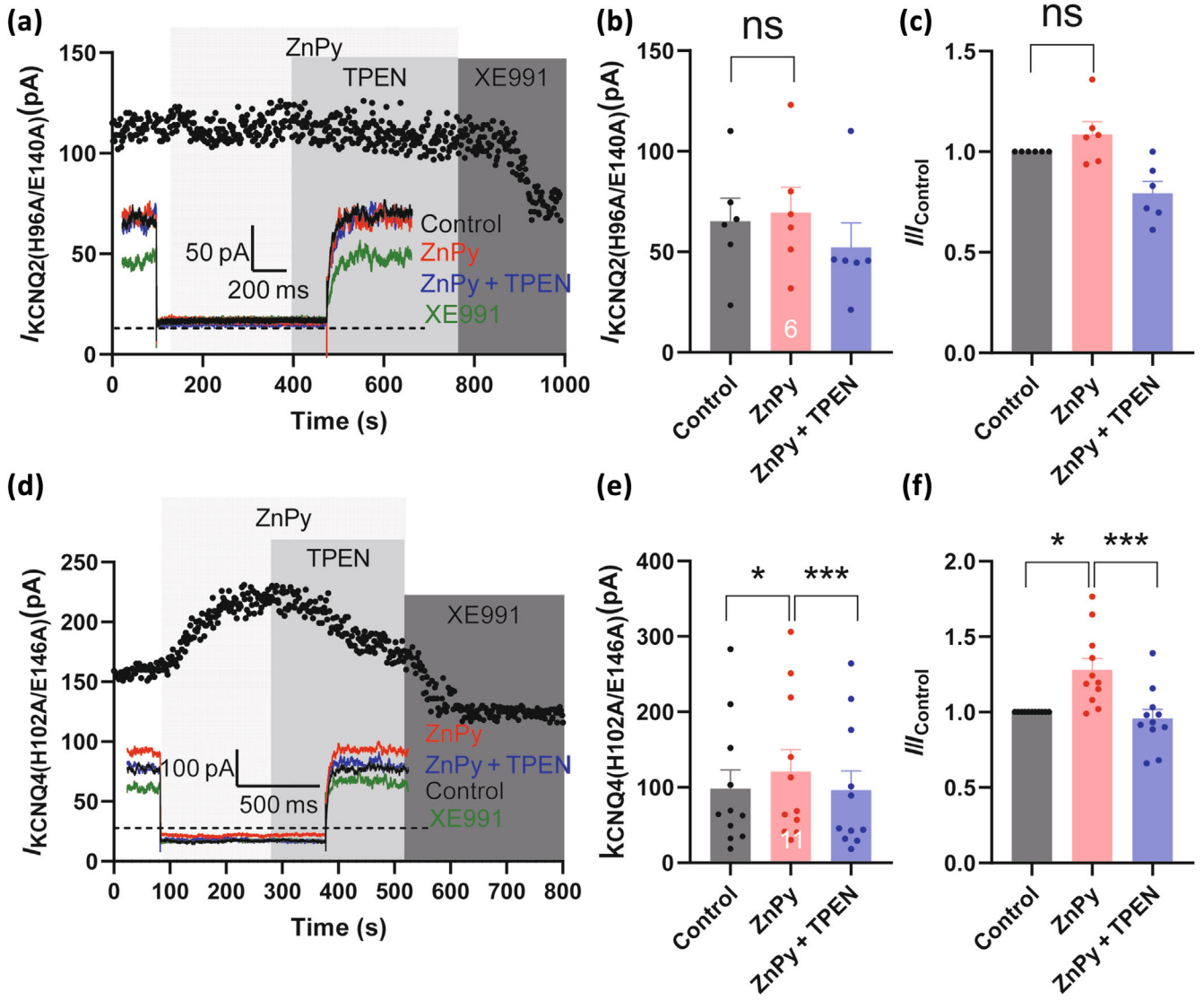

FIGURE 7 **Elucidation of the zinc coordination site in KCNQ2 and KCNQ4.** (a) Perforated patch-clamp recording from HEK293 cells transfected with *KCNQ2*(H96A/E140A). Time course of the effects of ZnPy (10 μM), TPEN (20 μM) and XE991 (10 mM) is shown. (b and c) Summaries of experiments shown in Figure 7a; number of experiments is indicated within the bars. Mean current amplitudes are summarised in Figure 7b, and normalised current amplitudes (relative to basal amplitude, $I_{control}$) are summarised in Figure 7c. (d) Perforated patch-clamp recording from HEK293 cells transfected with *KCNQ4*(H102A/E146A). Time course of the effects of ZnPy (10 μM), TPEN (20 μM) and XE991 (10 μM) is shown. (e and f) Summaries of experiments shown in Figure 7d; number of experiments is indicated within the bars. Mean current amplitudes are summarised in Figure 7e, and normalised current amplitudes (relative to basal amplitude, $I_{control}$) are summarised in Figure 7f. Asterisks depict significant difference between the groups indicated by connector lines; $^{*}P < 0.05$ and $^{***}P < 0.001$ (repeated-measures ANOVA with Bonferroni post hoc test or paired Student's *t*-test). ns, non-significant.

4 | DISCUSSION

4.1 | Zinc binding site of the KCNQ1 channel complex

In this study, we elucidated the zinc coordination site in KCNQ1, which is responsible for channel activation by intracellular Zn^{2+}. It is likely that this site is partially conserved across the KCNQ channel family (although with some significant differences; see succeeding text). We propose that in KCNQ1 the zinc binding site is located near the centre of the physical space for VSD and formed by H126 of the C-terminal end of S1, E170 at the cytosol-facing end of S2 and H240 of the S4–S5 linker. H126, E170 and H240 are directly involved in Zn^{2+} ion binding while D242 couples H240, via the rest of the S4–S5 linker, to the PD (S5–S6) (Figures 2a and 5g). Zn^{2+} binding to the H126-E170-H240 pocket produces a conformational signal, which facilitates channel opening. Mandala and MacKinnon recently reported structures of KCNQ1 in different conformations of the voltage-sensor region, revealing the molecular mechanism by which PIP_2 affects the voltage sensitivity of KCNQ1 (Mandala &

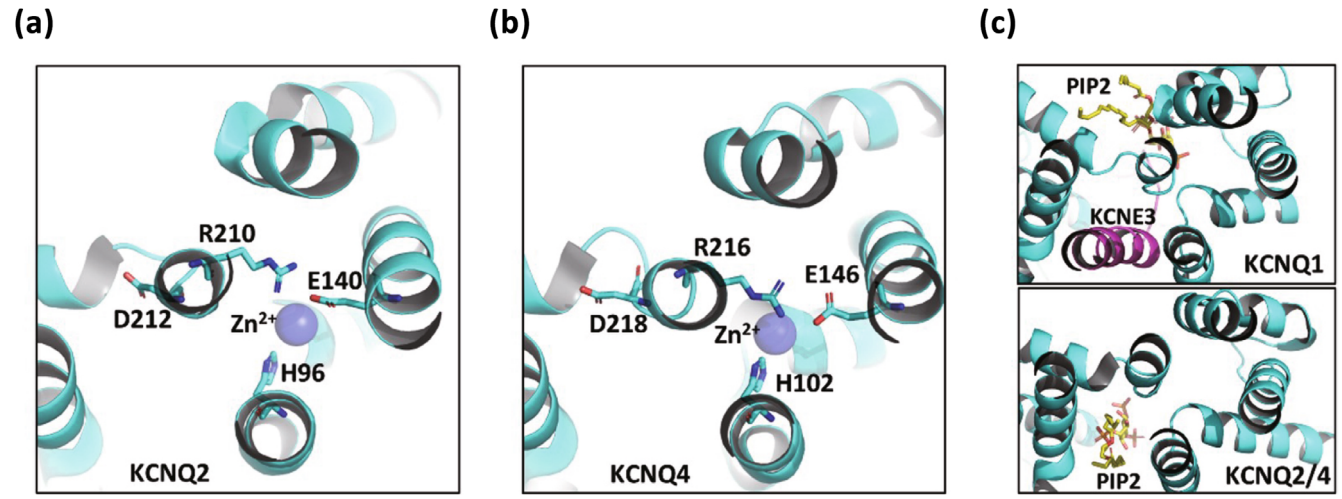

FIGURE 8 **Structural comparison of the putative zinc binding site regions of KCNQ1, KCNQ2 and KCNQ4**. (a and b) Zinc coordination sites of KCNQ2 (PDB ID: 7CR3) and KCNQ4 (PDB ID: 7BYL), respectively. (c) Differential position of PIP_2 relative to the VSD in KCNQ1, as compared to KCNQ2 and KCNQ4.

MacKinnon, 2023). This work identified H240 as a residue in the S4 helix that is positioned near the gating charge transfer centre and, thus, critical to voltage sensitivity. Our data suggest that H240 is involved in zinc coordination and, likely, the functional effect of zinc on channel gating. This indicates that H240 plays a dual regulatory role in voltage sensing and ligand regulation.

We further propose that incorporation of KCNE1 or KCNE3 into the WT KCNQ1 channel complex disturbs or blocks Zn^{2+} binding and/or current augmentation. Zinc-mediated partial current inhibition in this complex is likely to be mediated by a pore block.

Proximity between Zn^{2+}-binding and PIP_2-binding sites (Figures 2b and 8c) may explain previous observation that intracellular zinc elevation dramatically reduces or abolishes channel requirement for PIP_2 (Gao et al., 2017): we hypothesise that binding of Zn^{2+} to H126-E170-H240 pocket may stabilise the open state of the channel in a way similar to that by PIP_2.

4.2 | Putative role of D242

The most intriguing and difficult to reconcile result reported here was that mutation of D242 to a positively charged or hydrophobic residues abolished ZnPy-mediated activation of homomeric KCNQ1 channel (Figure 2), yet, when KCNQ1(D242A) was co-assembled with KCNE1 or KCNE3, the sensitivity to intracellular zinc was fully restored (Figure 3). Together with the observations that substitution of homologous aspartic acid in either KCNQ2 or KCNQ4 had no effect on the ability of zinc to activate these channels (Figure 6), these data suggest that (i) D242 is unlikely to participate in Zn^{2+} coordination directly but rather couples zinc binding to channel activation; (ii) this coupling role of D242 is unique to KCNQ1; and (iii) we further hypothesise that in the KCNQ1(D242A) mutant, insertion of KCNE1 or KCNE3 no longer sufficiently blocks Zn^{2+} binding to the core site (H126, E170 and H240), and such binding is able to produce a sufficient conformational change required to stabilise mutant channel open state, even in the absence of D242. The fact that D242A substitution strongly reduces the effect of KCNE1 binding on KCNQ1 voltage dependence (Figure S3) indirectly supports this idea.

We acknowledge that alternative explanations could exist, for instance, D242 and H126-E170-H240 may form separate (but coupled) Zn^{2+} binding sites. In such a scenario, Zn^{2+} occupancy at both sites would be required for the activation of WT KCNQ1 while incorporation of a KCNE subunit into the channel complex renders binding of Zn^{2+} to D242 redundant. But in any event, the role of D242 appears to be unique to KCNQ1 and does not play a significant role in Zn^{2+} modulation of other KCNQs tested here.

A previous study, investigating the effect of ZnPy on KCNQ1 channels, found that substitution of S6 residues, S338 and L342 with alanines abolished or inverted ZnPy-mediated activation of KCNQ1 (Z. Gao et al., 2008). These mutants were still sensitive to modulation by KCNE1/3. Likewise, several residues in KCNQ2 (L249, L275 and R306) were suggested to affect ZnPy sensitivity (Xiong et al., 2007). We hypothesise, that like D242, these mutations affect coupling of zinc binding to channel activation, rather than zinc binding itself. However, further research is needed to establish this.

4.3 | The zinc binding site in KCNQ2 and KCNQ4

Substitution of residues homologous to H126A, E170A and H240A of KCNQ1 in KCNQ4 and KCNQ2 resulted in channels that are no longer activated by zinc, suggesting that the core Zn^{2+} binding site in other KCNQ channels is relatively conserved. Yet, there is a number of significant differences: (i) as mentioned, aspartic acid at positions homologous to D242 of KCNQ1 is not important for the zinc effect in KCNQ2 and KCNQ4, probably reflecting structural differences in the S4–S5 linkers of KCNQ1 and the rest of the family (this linker in KCNQ1 is longer; Figure 6e). (ii) The position homologous to H240 in

KCNQ1 is occupied by arginine in all other KCNQ subunits, and this amino acid is less frequently associated with zinc coordination in proteins. However, a zinc-activated variant of human **carbonic anhydrase I** does contain arginine as a key zinc coordination residue (Ferraroni et al., 2002). (iii) Unlike KCNQ1, the rest of the family does not usually co-assemble with KCNE subunits (although such interactions were reported in the expression system; Tinel et al., 2000). (iv) According to the structural data available, the position of PIP_2 relative to zinc binding site in KCNQ1 (Sun & MacKinnon, 2020) is somewhat distinct, as compared to KCNQ2 (Ma et al., 2023) and KCNQ4 (Li et al., 2021), as depicted in Figure 8c. Hence, while all KCNQ channels can be activated by zinc (even KCNQ3, if its intrinsically high PIP_2 affinity is artificially reduced; Gao et al., 2017), the role of KCNE subunits and D242 in modulating zinc effects seems to be unique to KCNQ1.

4.4 | Structural divergence of the redox and zinc-mediated regulation of KCNQ channels

Interestingly, KCNQ channels are also activated by intracellular oxidisers, such as hydrogen peroxide (Abdullaeva et al., 2022; Gamper et al., 2006; Nuñez et al., 2023). A triplet of cysteines at the intracellular S2–S3 linker (Gamper et al., 2006; Ooi et al., 2013) and calmodulin (Nuñez et al., 2023) are required for this effect. As zinc often binds to cysteines (Vallee & Falchuk, 1993) and can be involved in redox modulation (Gamper & Ooi, 2015; Nelson et al., 2007), it was logical to expect that these two activation mechanisms would converge. For instance, **Cav3.2 T-type Ca^{2+} channels** are inhibited by both oxidising agents and zinc, and this modulation is structurally coupled via the high-affinity metal-binding 'Asp-Gly-His' motif formed by the extracellular IS1–IS2 and IS3–IS4 loops of domain I (Kang et al., 2010) and a group of extracellular cysteines present in the IS1–IS2 (Huang et al., 2016, 2020). Yet, in KCNQ channels, a redox-sensitive module is apparently distinct from the zinc-coordination site as removal of all cysteines in the S2–S3 linker in KCNQ4 completely abolished redox sensitivity but had no effect on the ability of intracellular zinc to activate the channel (Gamper et al., 2006; Gao et al., 2017; Nuñez et al., 2023; Ooi et al., 2013). Although structurally distinct, the activating effects of zinc and oxidisers could converge elsewhere, for instance, by reducing channel PIP_2 requirement; however, further research is needed to investigate this matter.

4.5 | Clinical relevance

KCNQ channels are effective regulators of neuronal and muscle cell excitability and are a validated drug target for treatment of excitability disorders. (Du et al., 2018; Jones et al., 2021; Liu et al., 2021; Perucca & Taglialatela, 2025). Importantly, first-generation Kv7 channel activators, **retigabine** and **flupirtine**, have been successfully used clinically as an anticonvulsant (retigabine) and an analgesic (flupirtine) (Bock & Link, 2019; Clark et al., 2015). Even though the use of both drugs is currently restricted because of a range of side effects, their undisputed clinical efficacy triggered an industry-wide search for better analogues. Our data highlighted a structural mechanism, whereby intracellular zinc can stabilise KCNQ channel opening and reduce its requirement of PIP_2. The latter aspect can help develop KCNQ activators, which could protect channel activity against physiological inhibition by neurotransmitters and neuromodulators that deplete PIP_2 via the phospholipase C pathways, such as **acetylcholine**, **angiotensin II** and **bradykinin** (Delmas & Brown, 2005; Hernandez et al., 2008). Such an approach can pave way to activity-dependent KCNQ modulators, which would protect against neuronal hyperactivity with weaker effects in less active neural tissue, limiting side effects.

4.6 | Limitations

Some of the mutants generated in this study exhibited very small current amplitudes. Although these currents remained responsive to their respective activators and inhibitors, their low magnitude, combined with the contribution of endogenous ion channels in CHO and HEK293 cells, made the analysis of zinc sensitivity of these mutants less precise.

4.7 | Conclusions

In sum, we report a partially conserved zinc coordination site of KCNQ channels assembled at the cytosolic interface of the channel complex and responsible for potent activating effect of intracellular Zn^{2+}. Given high therapeutic value of KCNQ channel openers for treatment of excitability disorders (Gamper & Shapiro, 2015; Jones et al., 2021; Liu et al., 2021; Perucca & Taglialatela, 2025), this structural insight may help future drug design.

AUTHOR CONTRIBUTIONS

N. Gamper, H. Gao and **S. Shi**: Conceptualisation. **S. Zhang, X. Yang, M. Yang** and **Y. Cao**: Investigation. **N. Gamper**: Writing—original draft. **N. Gamper, S. Zhang, S. Shi** and **H. Gao**: Writing—review and editing. **S. Zhang, X. Yang** and **S. Shi**: Visualisation. **N. Gamper** and **H. Gao**: Supervision. **H. Gao, S. Shi** and **N. Gamper**: Funding acquisition.

ACKNOWLEDGEMENTS

This work was supported by the National Natural Science Foundation of China grant (81871027) to H.G. and N.G.; the Hebei Province Talent and Intelligence Introduction Project Award to H.G. and N.G.; Central Guiding Local Science and Technology Development Fund Project (236Z7723G) to H.G.; Hebei Natural Science Foundation award (H2022206515) to H.G.; Key laboratory of Neural and Vascular Biology, Ministry of Education of China project NV20230001 to H.G.; the National Natural Science Foundation of China to S.S. (82404583); and the Biotechnology and Biological Sciences Research Council grants BB/V010344/1 and BB/R02104X/1 to N.G. This research was supported by the Medical Science Data Center of Hebei Medical University.

CONFLICT OF INTEREST STATEMENT

The authors declare no conflicts of interest.

DATA AVAILABILITY STATEMENT

The data that support the findings of this study are available from the corresponding author upon reasonable request. Some data may not be made available because of privacy or ethical restrictions.

DECLARATION OF TRANSPARENCY AND SCIENTIFIC RIGOUR

This Declaration acknowledges that this paper adheres to the principles for transparent reporting and scientific rigour of preclinical research as stated in the *BJP* guidelines for Design and Analysis, and as recommended by funding agencies, publishers and other organisations engaged with supporting research.

ORCID

Nikita Gamper https://orcid.org/0000-0001-5806-0207

REFERENCES

Abbott, G. W. (2020). KCNQs: Ligand- and voltage-gated potassium channels. *Frontiers in Physiology*, *11*, 583. https://doi.org/10.3389/fphys.2020.00583

Abbott, G. W. (2021). Control of biophysical and pharmacological properties of potassium channels by ancillary subunits. *Handbook of Experimental Pharmacology*, *267*, 445–480. https://doi.org/10.1007/164_2021_512

Abdullaeva, O. S., Sahalianov, I., Silvera Ejneby, M., Jakesova, M., Zozoulenko, I., Liin, S. I., & Glowacki, E. D. (2022). Faradaic pixels for precise hydrogen peroxide delivery to control m-type voltage-gated potassium channels. *Advanced Science (Weinh)*, *9*(3), e2103132. https://doi.org/10.1002/advs.202103132

Alberts, I. L., Nadassy, K., & Wodak, S. J. (1998). Analysis of zinc binding sites in protein crystal structures. *Protein Science*, *7*(8), 1700–1716. https://doi.org/10.1002/pro.5560070805

Alexander, S. P., Mathie, A. A., Peters, J. A., Veale, E. L., Striessnig, J., Kelly, E., Armstrong, J. F., Faccenda, E., Harding, S. D., Davies, J. A., Aldrich, R. W., Attali, B., Baggetta, A. M., Becirovic, E., Biel, M., Bill, R. M., Caceres, A. I., Catterall, W. A., Conner, A. C., … Zhu, M. (2023). The concise guide to PHARMACOLOGY 2023/24: Ion channels. *British Journal of Pharmacology*, *180*, S145–S222. https://doi.org/10.1111/bph.16178

Alexander, S. P. H., Christopoulos, A., Davenport, A. P., Kelly, E., Mathie, A. A., Peters, J. A., Veale, E. L., Armstrong, J. F., Faccenda, E., Harding, S. D., Davies, J. A., Abbracchio, M. P., Abraham, G., Agoulnik, A., Alexander, W., Al-Hosaini, K., Bäck, M., Baker, J. G., Barnes, N. M., … Ye, R. D. (2023). The Concise Guide to PHARMACOLOGY 2023/24: G protein-coupled receptors. *British Journal of Pharmacology*, *180*, S23–S144. https://doi.org/10.1111/bph.16177

Alexander, S. P. H., Fabbro, D., Kelly, E., Mathie, A. A., Peters, J. A., Veale, E. L., Armstrong, J. F., Faccenda, E., Harding, S. D., Davies, J. A., Annett, S., Boison, D., Burns, K. E., Dessauer, C., Gertsch, J., Helsby, N. A., Izzo, A. A., Ostrom, R., Papapetropoulos, A., … Wong, S. S. (2023). The concise guide to PHARMACOLOGY 2023/24: Enzymes. *British Journal of Pharmacology*, *180*, S289–S373. https://doi.org/10.1111/bph.16181

Barhanin, J., Lesage, F., Guillemare, E., Fink, M., Lazdunski, M., & Romey, G. (1996). K(V)LQT1 and IsK (minK) proteins associate to form the I (Ks) cardiac potassium current. *Nature*, *384*(6604), 78–80. https://doi.org/10.1038/384078a0

Barrese, V., Stott, J. B., & Greenwood, I. A. (2018). KCNQ-encoded potassium channels as therapeutic targets. *Annual Review of Pharmacology and Toxicology*, *58*, 625–648. https://doi.org/10.1146/annurev-pharmtox-010617-052912

Bendahhou, S., Marionneau, C., Haurogne, K., Larroque, M. M., Derand, R., Szuts, V., Escande, D., Demolombe, S., & Barhanin, J. (2005). In vitro molecular interactions and distribution of KCNE family with KCNQ1 in the human heart. *Cardiovascular Research*, *67*(3), 529–538. https://doi.org/10.1016/j.cardiores.2005.02.014

Blakemore, L. J., & Trombley, P. Q. (2017). Zinc as a neuromodulator in the central nervous system with a focus on the olfactory bulb. *Frontiers in Cellular Neuroscience*, *11*, 297. https://doi.org/10.3389/fncel.2017.00297

Bock, C., & Link, A. (2019). How to replace the lost keys? Strategies toward safer K(V)7 channel openers. *Future Medicinal Chemistry*, *11*(4), 337–355. https://doi.org/10.4155/fmc-2018-0350

Borgini, M., Mondal, P., Liu, R., & Wipf, P. (2021). Chemical modulation of Kv7 potassium channels. *RSC Medicinal Chemistry*, *12*(4), 483–537. https://doi.org/10.1039/d0md00328j

Brown, D. A., & Adams, P. R. (1980). Muscarinic suppression of a novel voltage-sensitive K+ current in a vertebrate neurone. *Nature*, *283*(5748), 673–676. https://doi.org/10.1038/283673a0

Brown, D. A., & Passmore, G. M. (2009). Neural KCNQ (Kv7) channels. *British Journal of Pharmacology*, *156*(8), 1185–1195. https://doi.org/10.1111/j.1476-5381.2009.00111.x

Clark, S., Antell, A., & Kaufman, K. (2015). New antiepileptic medication linked to blue discoloration of the skin and eyes. *Therapeutic Advances in Drug Safety*, *6*(1), 15–19. https://doi.org/10.1177/2042098614560736

Curtis, M. J., Alexander, S. P. H., Cortese-Krott, M., Kendall, D. A., Martemyanov, K. A., Mauro, C., Panettieri, R. A. Jr., Papapetropoulos, A., Patel, H. H., Santo, E. E., Schulz, R., Stefanska, B., Stephens, G. J., Teixeira, M. M., Vergnolle, N., Wang, X., & Ferdinandy, P. (2025). Guidance on the planning and reporting of experimental design and analysis. *British Journal of Pharmacology*, *182*(7), 1413–1415. https://doi.org/10.1111/bph.17441

Delmas, P., & Brown, D. A. (2005). Pathways modulating neural KCNQ/M (Kv7) potassium channels. *Nature Reviews. Neuroscience*, *6*, 850–862. https://doi.org/10.1038/nrn1785

Dorward, A. M., Stewart, A. J., & Pitt, S. J. (2023). The role of Zn2+ in shaping intracellular Ca2+ dynamics in the heart. *The Journal of General Physiology*, *155*(7), e202213206. https://doi.org/10.1085/jgp.202213206

Du, X., Gao, H., Jaffe, D., Zhang, H., & Gamper, N. (2018). M-type K+ channels in peripheral nociceptive pathways. *British Journal of Pharmacology*, *175*, 2158–2172. https://doi.org/10.1111/bph.13978

Ferraroni, M., Tilli, S., Briganti, F., Chegwidden, W. R., Supuran, C. T., Wiebauer, K. E., Tashian, R. E., & Scozzafava, A. (2002). Crystal structure of a zinc-activated variant of human carbonic anhydrase I, CA I Michigan 1: Evidence for a second zinc binding site involving arginine coordination. *Biochemistry*, *41*(20), 6237–6244. https://doi.org/10.1021/bi0120446

Gamper, N., & Ooi, L. (2015). Redox and nitric oxide-mediated regulation of sensory neuron ion channel function. *Antioxidants & Redox Signaling*, *22*(6), 486–504. https://doi.org/10.1089/ars.2014.5884

Gamper, N., & Shapiro, M. S. (2015). KCNQ Channels. In J. Zheng & M. C. Trudeau (Eds.), *Handbook of ion channels* (pp. 275–306). CRC Press.

Gamper, N., Zaika, O., Li, Y., Martin, P., Hernandez, C. C., Perez, M. R., Wang, A. Y., Jaffe, D. B., & Shapiro, M. S. (2006). Oxidative modification of M-type K(+) channels as a mechanism of cytoprotective neuronal silencing. *The EMBO Journal*, *25*(20), 4996–5004. https://doi.org/10.1038/sj.emboj.7601374

Gao, H., Boillat, A., Huang, D., Liang, C., Peers, C., & Gamper, N. (2017). Intracellular zinc activates KCNQ channels by reducing their dependence on phosphatidylinositol 4,5-bisphosphate. *Proceedings of the*

National Academy of Sciences of the United States of America, *114*(31), E6410–E6419. https://doi.org/10.1073/pnas.1620598114

Gao, Z., Xiong, Q., Sun, H., & Li, M. (2008). Desensitization of chemical activation by auxiliary subunits: convergence of molecular determinants critical for augmenting KCNQ1 potassium channels. *The Journal of Biological Chemistry*, *283*(33), 22649–22658. https://doi.org/10.1074/jbc.M802426200

Greene, D. L., & Hoshi, N. (2016). Modulation of Kv7 channels and excitability in the brain. *Cellular and Molecular Life Sciences*, *74*, 495–508. https://doi.org/10.1007/s00018-016-2359-y

Hamilton, K. L., & Devor, D. C. (2012). Basolateral membrane K+ channels in renal epithelial cells. *American Journal of Physiology. Renal Physiology*, *302*(9), F1069–F1081. https://doi.org/10.1152/ajprenal.00646.2011

Hernandez, C. C., Zaika, O., Tolstykh, G. P., & Shapiro, M. S. (2008). Regulation of neural KCNQ channels: signalling pathways, structural motifs and functional implications. *The Journal of Physiology*, *586*(7), 1811–1821. https://doi.org/10.1113/jphysiol.2007.148304

Huang, D., Huang, S., Gao, H., Liu, Y., Qi, J., Chen, P., Wang, C., Scragg, J. L., Vakurov, A., Peers, C., Du, X., Zhang, H., & Gamper, N. (2016). Redox-dependent modulation of T-type Ca(2+) channels in sensory neurons contributes to acute anti-nociceptive effect of substance P. *Antioxidants & Redox Signaling*, *25*(5), 233–251. https://doi.org/10.1089/ars.2015.6560

Huang, D., Shi, S., Liang, C., Zhang, X., Du, X., An, H., Peers, C., Zhang, H., & Gamper, N. (2020). Delineating an extracellular redox-sensitive module in T-type Ca(2+) channels. *The Journal of Biological Chemistry*, *295*(18), 6177–6186. https://doi.org/10.1074/jbc.RA120.012668

Jones, F., Gamper, N., & Gao, H. (2021). Kv7 Channels and excitability disorders. *Handbook of Experimental Pharmacology*, *267*, 185–230. https://doi.org/10.1007/164_2021_457

Kambe, T., Tsuji, T., & Fukue, K. (2014). Zinc transport porteins and zinc signaling. In T. Fukada & T. Kambe (Eds.), *Zinc signals in cellular functions and disorders* (pp. 27–53). Springer. https://doi.org/10.1007/978-4-431-55114-0_3

Kambe, T., Tsuji, T., Hashimoto, A., & Itsumura, N. (2015). The physiological, biochemical, and molecular roles of zinc transporters in zinc homeostasis and metabolism. *Physiological Reviews*, *95*(3), 749–784. https://doi.org/10.1152/physrev.00035.2014

Kang, H. W., Vitko, I., Lee, S. S., Perez-Reyes, E., & Lee, J. H. (2010). Structural determinants of the high affinity extracellular zinc binding site on Cav3.2 T-type calcium channels. *The Journal of Biological Chemistry*, *285*(5), 3271–3281. https://doi.org/10.1074/jbc.M109.067660

Kapplinger, J. D., Tseng, A. S., Salisbury, B. A., Tester, D. J., Callis, T. E., Alders, M., Wilde, A. A., & Ackerman, M. J. (2015). Enhancing the predictive power of mutations in the C-terminus of the KCNQ1-encoded Kv7.1 voltage-gated potassium channel. *Journal of Cardiovascular Translational Research*, *8*(3), 187–197. https://doi.org/10.1007/s12265-015-9622-8

Kottgen, M., Hoefer, A., Kim, S. J., Beschorner, U., Schreiber, R., Hug, M. J., & Greger, R. (1999). Carbachol activates a K+ channel of very small conductance in the basolateral membrane of rat pancreatic acinar cells. *Pflügers Archiv*, *438*(5), 597–603. https://doi.org/10.1007/s004249900070

Li, T., Wu, K., Yue, Z., Wang, Y., Zhang, F., & Shen, H. (2021). Structural basis for the modulation of human KCNQ4 by small-molecule drugs. *Molecular Cell*, *81*(1), 25–37 e24. https://doi.org/10.1016/j.molcel.2020.10.037

Liu, Y., Bian, X., & Wang, K. (2021). Pharmacological activation of neuronal voltage-gated Kv7/KCNQ/M-channels for potential therapy of epilepsy and pain. *Handbook of Experimental Pharmacology*, *267*, 231–251. https://doi.org/10.1007/164_2021_458

Ma, D., Zheng, Y., Li, X., Zhou, X., Yang, Z., Zhang, Y., Wang, L., Zhang, W., Fang, J., Zhao, G., Hou, P., Nan, F., Yang, W., Su, N., Gao, Z., & Guo, J. (2023). Ligand activation mechanisms of human KCNQ2 channel. *Nature Communications*, *14*(1), 6632. https://doi.org/10.1038/s41467-023-42416-x

Mandala, V. S., & MacKinnon, R. (2023). The membrane electric field regulates the PIP(2)-binding site to gate the KCNQ1 channel. *Proceedings of the National Academy of Sciences of the United States of America*, *120*(21), e2301985120. https://doi.org/10.1073/pnas.2301985120

Mattmann, M. E., Yu, H., Lin, Z., Xu, K., Huang, X., Long, S., Wu, M., McManus, O. B., Engers, D. W., Le, U. M., Li, M., Lindsley, C. W., & Hopkins, C. R. (2012). Identification of (R)-N-(4-[4-methoxyphenyl] thiazol-2-yl)-1-tosylpiperidine-2-carboxamide, ML277, as a novel, potent and selective K(v)7.1 (KCNQ1) potassium channel activator. *Bioorganic & Medicinal Chemistry Letters*, *22*(18), 5936–5941. https://doi.org/10.1016/j.bmcl.2012.07.060

Mousavi Nik, A., Gharaie, S., & Jeong Kim, H. (2015). Cellular mechanisms of mutations in Kv7.1: auditory functions in Jervell and Lange-Nielsen syndrome vs. Romano-Ward syndrome. *Frontiers in Cellular Neuroscience*, *9*, 32. https://doi.org/10.3389/fncel.2015.00032

Nelson, M. T., Joksovic, P. M., Su, P., Kang, H. W., Van Deusen, A., Baumgart, J. P., David, L. S., Snutch, T. P., Barrett, P. Q., Lee, J. H., Zorumski, C. F., Perez-Reyes, E., & Todorovic, S. M. (2007). Molecular mechanisms of subtype-specific inhibition of neuronal T-type calcium channels by ascorbate. *The Journal of Neuroscience*, *27*(46), 12577–12583. https://doi.org/10.1523/JNEUROSCI.2206-07.2007

Nicolas, C. S., Park, K. H., El Harchi, A., Camonis, J., Kass, R. S., Escande, D., Mérot, J., Loussouarn, G., Le Bouffant, F., & Baró, I. (2008). IKs response to protein kinase A-dependent KCNQ1 phosphorylation requires direct interaction with microtubules. *Cardiovascular Research*, *79*(3), 427–435. https://doi.org/10.1093/cvr/cvn085

Nuñez, E., Jones, F., Muguruza-Montero, A., Urrutia, J., Aguado, A., Malo, C., Bernardo-Seisdedos, G., Domene, C., Millet, O., Gamper, N., & Villarroel, A. (2023). Redox regulation of K(v)7 channels through EF3 hand of calmodulin. *eLife*, *12*, e81961. https://doi.org/10.7554/eLife.81961

Oertli, A., Rinne, S., Moss, R., Kaab, S., Seemann, G., Beckmann, B. M., & Decher, N. (2021). Molecular mechanism of autosomal recessive long QT-syndrome 1 without deafness. *International Journal of Molecular Sciences*, *22*(3), 1112. https://doi.org/10.3390/ijms22031112

Ooi, L., Gigout, S., Pettinger, L., & Gamper, N. (2013). Triple cysteine module within M-type K+ channels mediates reciprocal channel modulation by nitric oxide and reactive oxygen species. *The Journal of Neuroscience*, *33*(14), 6041–6046. https://doi.org/10.1523/JNEUROSCI.4275-12.2013

Perucca, E., & Taglialatela, M. (2025). Targeting Kv7 potassium channels for epilepsy. *CNS Drugs*, *39*(3), 263–288. https://doi.org/10.1007/s40263-024-01155-3

Reilly-O'Donnell, B., Robertson, G. B., Karumbi, A., McIntyre, C., Bal, W., Nishi, M., Takeshima, H., Stewart, A. J., & Pitt, S. J. (2017). Dysregulated Zn(2+) homeostasis impairs cardiac type-2 ryanodine receptor and mitsugumin 23 functions, leading to sarcoplasmic reticulum Ca(2+) leakage. *The Journal of Biological Chemistry*, *292*(32), 13361–13373. https://doi.org/10.1074/jbc.M117.781708

Robbins, J. (2001). KCNQ potassium channels: Physiology, pathophysiology, and pharmacology. *Pharmacology & Therapeutics*, *90*(1), 1–19. https://doi.org/10.1016/s0163-7258(01)00116-4

Sanguinetti, M. C., Curran, M. E., Zou, A., Shen, J., Spector, P. S., Atkinson, D. L., & Keating, M. T. (1996). Coassembly of K(V)LQT1 and minK (IsK) proteins to form cardiac I (Ks) potassium channel. *Nature*, *384*(6604), 80–83. https://doi.org/10.1038/384080a0

Scavo, S., & Oliveri, V. (2022). Zinc ionophores: Chemistry and biological applications. *Journal of Inorganic Biochemistry*, *228*, 111691. https://doi.org/10.1016/j.jinorgbio.2021.111691

Schreiber, J. A., & Seebohm, G. (2021). Cardiac K(+) channels and channelopathies. *Handbook of Experimental Pharmacology*, *267*, 113–138. https://doi.org/10.1007/164_2021_513

Schroeder, B. C., Waldegger, S., Fehr, S., Bleich, M., Warth, R., Greger, R., & Jentsch, T. J. (2000). A constitutively open potassium channel formed by KCNQ1 and KCNE3. *Nature*, *403*(6766), 196–199. https://doi.org/10.1038/35003200

Stott, J. B., Jepps, T. A., & Greenwood, I. A. (2014). K(V)7 potassium channels: A new therapeutic target in smooth muscle disorders. *Drug Discovery Today*, *19*(4), 413–424. https://doi.org/10.1016/j.drudis.2013.12.003

Sun, J., & MacKinnon, R. (2020). Structural basis of human KCNQ1 modulation and gating. *Cell*, *180*(2), 340–347 e349. https://doi.org/10.1016/j.cell.2019.12.003

Takeda, A. (2014). Significance of Zn(2+) signaling in cognition: insight from synaptic Zn(2+) dyshomeostasis. *Journal of Trace Elements in Medicine and Biology*, *28*(4), 393–396. https://doi.org/10.1016/j.jtemb.2014.06.021

Thomas, G. P., Gerlach, U., & Antzelevitch, C. (2003). HMR 1556, a potent and selective blocker of slowly activating delayed rectifier potassium current. *Journal of Cardiovascular Pharmacology*, *41*(1), 140–147. https://doi.org/10.1097/00005344-200301000-00018

Tinel, N., Diochot, S., Lauritzen, I., Barhanin, J., Lazdunski, M., & Borsotto, M. (2000). M-type KCNQ2-KCNQ3 potassium channels are modulated by the KCNE2 subunit. *FEBS Letters*, *480*(2–3), 137–141. https://doi.org/10.1016/s0014-5793(00)01918-9

Turan, B., Fliss, H., & Desilets, M. (1997). Oxidants increase intracellular free Zn2+ concentration in rabbit ventricular myocytes. *The American Journal of Physiology*, *272*(5 Pt 2), H2095–H2106. https://doi.org/10.1152/ajpheart.1997.272.5.H2095

Ullrich, S., Su, J., Ranta, F., Wittekindt, O. H., Ris, F., Rösler, M., Gerlach, U., Heitzmann, D., Warth, R., & Lang, F. (2005). Effects of I (Ks) channel inhibitors in insulin-secreting INS-1 cells. *Pflügers Archiv*, *451*(3), 428–436. https://doi.org/10.1007/s00424-005-1479-2

Unoki, H., Takahashi, A., Kawaguchi, T., Hara, K., Horikoshi, M., Andersen, G., Ng, D. P., Holmkvist, J., Borch-Johnsen, K., Jørgensen, T., Sandbaek, A., Lauritzen, T., Hansen, T., Nurbaya, S., Tsunoda, T., Kubo, M., Babazono, T., Hirose, H., Hayashi, M., … Maeda, S. (2008). SNPs in KCNQ1 are associated with susceptibility to type 2 diabetes in East Asian and European populations. *Nature Genetics*, *40*(9), 1098–1102. https://doi.org/10.1038/ng.208

Upmanyu, N., Jin, J., Emde, H. V., Ganzella, M., Bösche, L., Malviya, V. N., Zhuleku, E., Politi, A. Z., Ninov, M., Silbern, I., Leutenegger, M., Urlaub, H., Riedel, D., Preobraschenski, J., Milosevic, I., Hell, S. W., Jahn, R., & Sambandan, S. (2022). Colocalization of different neurotransmitter transporters on synaptic vesicles is sparse except for VGLUT1 and ZnT3. *Neuron*, *110*(9), 1483–1497 e1487. https://doi.org/10.1016/j.neuron.2022.02.008

Vallee, B. L., & Falchuk, K. H. (1993). The biochemical basis of zinc physiology. *Physiological Reviews*, *73*(1), 79–118. https://doi.org/10.1152/physrev.1993.73.1.79

Vallon, V., Grahammer, F., Volkl, H., Sandu, C. D., Richter, K., Rexhepaj, R., Gerlach, U., Rong, Q., Pfeifer, K., & Lang, F. (2005). KCNQ1-dependent transport in renal and gastrointestinal epithelia. *Proceedings of the National Academy of Sciences of the United States of America*, *102*(49), 17864–17869. https://doi.org/10.1073/pnas.0505860102

van der Horst, J., Greenwood, I. A., & Jepps, T. A. (2020). Cyclic AMP-Dependent Regulation of Kv7 Voltage-Gated Potassium Channels. *Frontiers in Physiology*, *11*, 727. https://doi.org/10.3389/fphys.2020.00727

Wang, J. J., & Li, Y. (2016). KCNQ potassium channels in sensory system and neural circuits. *Acta Pharmacologica Sinica*, *37*(1), 25–33. https://doi.org/10.1038/aps.2015.131

Xiong, Q., Sun, H., & Li, M. (2007). Zinc pyrithione-mediated activation of voltage-gated KCNQ potassium channels rescues epileptogenic mutants. *Nature Chemical Biology*, *3*(5), 287–296. https://doi.org/10.1038/nchembio874

Yang, X., Chen, S., Zhang, S., Shi, S., Zong, R., Gao, Y., Guan, B., Gamper, N., & Gao, H. (2023). Intracellular zinc protects Kv7 K(+) channels from Ca(2+)/calmodulin-mediated inhibition. *The Journal of Biological Chemistry*, *299*(2), 102819. https://doi.org/10.1016/j.jbc.2022.102819

Zhang, J., Juhl, C. R., Hylten-Cavallius, L., Salling-Olsen, M., Linneberg, A., Holst, J. J., Hansen, T., Kanters, J. K., & Torekov, S. S. (2020). Gain-of-function mutation in the voltage-gated potassium channel gene KCNQ1 and glucose-stimulated hypoinsulinemia—Case report. *BMC Endocrine Disorders*, *20*(1), 38. https://doi.org/10.1186/s12902-020-0513-x

SUPPORTING INFORMATION

Additional supporting information can be found online in the Supporting Information section at the end of this article.

How to cite this article: Zhang, S., Yang, X., Yang, M., Cao, Y., Shi, S., Gamper, N., & Gao, H. (2025). Elucidation of the zinc binding site in KCNQ channels. *British Journal of Pharmacology*, 1–19. https://doi.org/10.1111/bph.70177